Molecular Dynamics Simulations of resistin and RELMβ proteins: Insight into structural dynamics.

L. América Chi[1] and M. Cristina Vargas[1]

[1]*Departamento de Física Aplicada, Centro de Investigación y de Estudios Avanzados del Instituto Politécnico Nacional, Unidad Mérida. Apartado Postal 73 "Cordemex", 97310, Mérida, Yucatán, México.*

Email: america.chi@cinvestav.mx, cristina.vargas@cinvestav.mx

Abstract

Diabetes mellitus and high levels of resistin are risk factors for COVID-19, suggesting a shared mechanism for their contribution to the increased severity of COVID-19. Resistin belongs to the family of resistin-like molecules (RELMs) whose implications for inflammatory and metabolic dysfunctions warrant its study in order to shed light on the etiology of these concerning pathologies. In this work, our objective is to characterize the structural dynamics of the reported crystallized resistin-like molecules. We performed molecular dynamics simulations of all-atom solvated protein at physiological and high temperatures for the three mouse structures reported so far. We found that in all the structures studied, there is a loss of helicity as a first step of protein denaturation. There is a high stability of the globular β-sheet domain in resistin protein structures that is not conserved for RELMβ. At high temperature, we found a partial interconversion of α-helices into β-sheets in all proteins, indicating that this propensity is not only found during aggregation but also heating. We had been able to identify a largely persistent hydrogen-bond network shared by all the proteins in the interchain globular domain at room temperature. This network of hydrogen bonds is conserved considerably at high temperature in resistin structures, but not in RELMβ. These findings may guide future studies to increase our understanding of the different and shared mechanisms of action of RELMs.

1 Introduction

The family of Resistin Like Molecules (RELMs) are cysteine-rich proteins that are exclusively secreted in mammals. They contain three domains [1]: i) an N-terminal signal sequence, ii) a variable middle portion, and iii) a highly conserved C-terminal signature sequence (C-X_{11}-C-X_8-CX-C-X_3-C-X_{10}-C-X-C-X-C-X_9-CC-X_{3-6}-END, where X states for any other amino acid different from cysteine and the subindices represent the number of amino acids between cysteines). The members of this family are resistin, RELMβ, RELMα, and RELMγ. Although all the members have been found in rodents, only resistin and RELMβ homologs have so far been seen in humans. The primary sequence and structure of representative members of this family are displayed in Figure 1 and Figure 2. The RELMs have been involved in a wide variety of biological processes, which can be divided into 2 types mainly: i) Inflammatory diseases, including, liver diseases [2], lung diseases [3], atherosclerosis [4], kidney diseases [5], intestinal diseases [6], cancer [7], cardiovascular diseases [8], autoimmune diseases [9], and asthma [10]; and ii) Metabolic dysfunctions, including Diabetes Mellitus Type 2 (T2DM) [1], hyperlipidemia [11] and insulin resistance (IR) [12]; among others [13–15]. Recently, resistin was identified as a causal risk factor of severe coronavirus disease 2019 (COVID-19) [16, 17]. The relationships of the RELMs with this broad range of pathological environments highlights the important physiological role they play.

One of the first results that attracted attention towards the RELMs was the suggestion of resistin member as a potential link between obesity and IR, both related to DMT2. This result was supported by the following facts in rodents: i) Resistin level is increased in genetic and diet-induced obesity, ii) The inhibition or genetic suppression of resistin produced an increase in insulin sensitivity and glucose homeostasis, and iii) Inverse administration of exogenous or transgenic resistin,

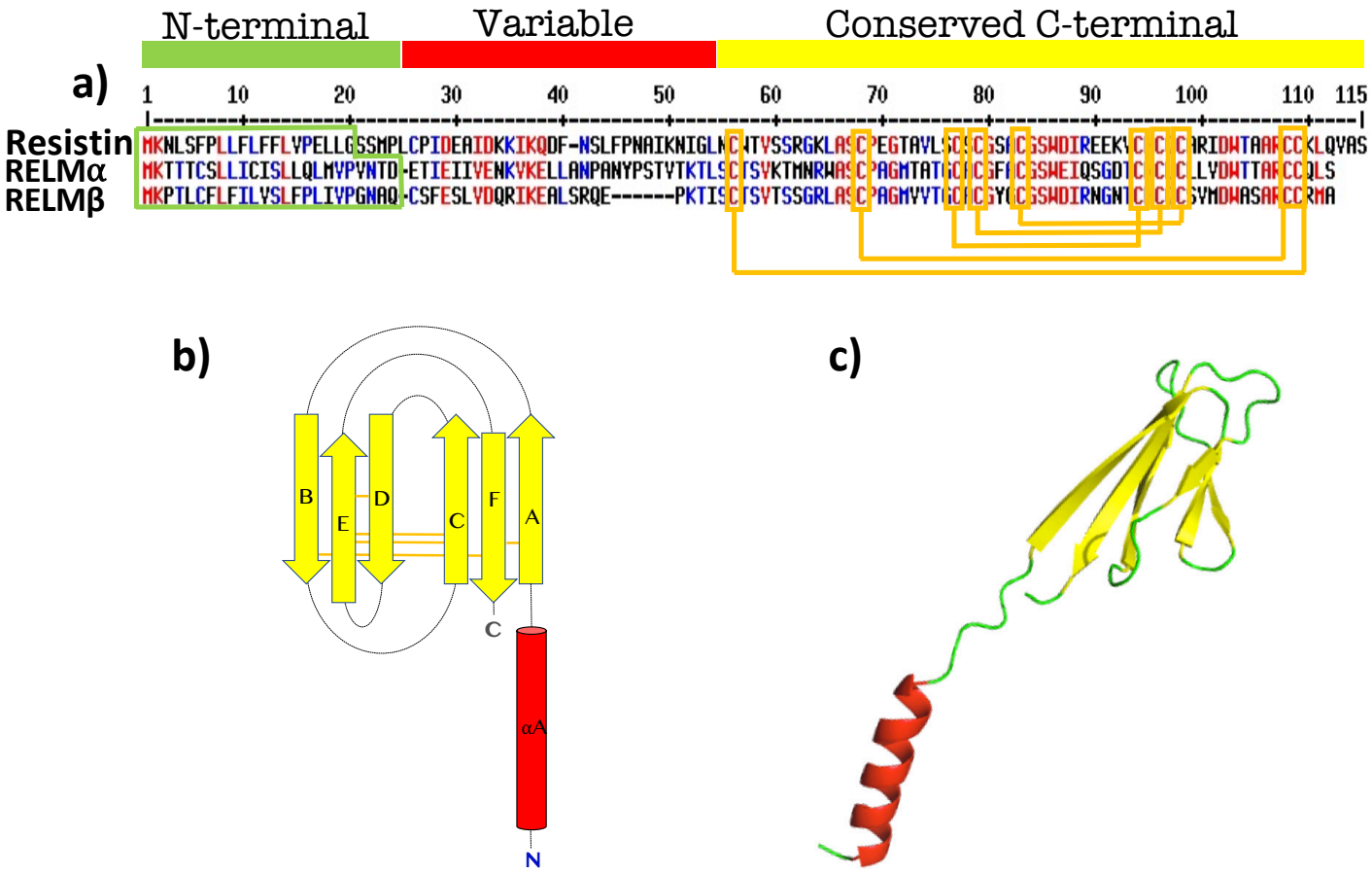

Figure 1: Structure of mouse RELMs. a) Primary sequence alignment of different RELMs (green box represents the signal peptide, orange box the conserved cysteines, orange lines represent disulfide bonds and amino acids are represented with standard one-letter code), b) folding topology (the yellow arrows represent beta-sheet secondary structures, red cilinders represent helical structures and orange lines represent disulfide bonds) and c) tertiary structure.

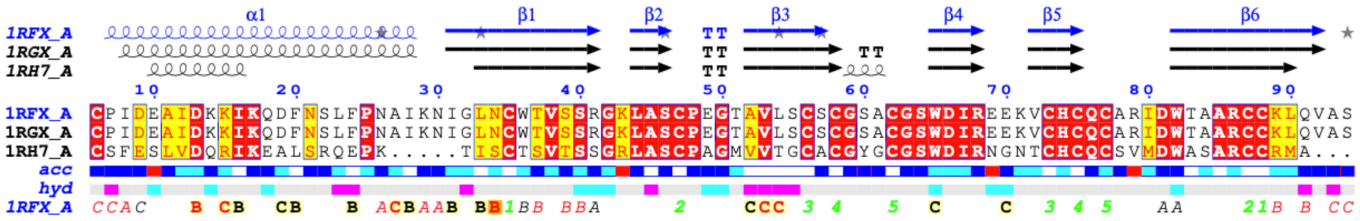

Figure 2: Secondary structure of mouse resistin(PDBID:1rfx,1rgx) and mouse RELMβ(PDBID:1rh7) crystal structures reported in Protein Data Bank(PDB) [32]. The secondary structure is assigned by DSSP algorithm through ENDscript 2.0 program [33] for Chain A. α-helices are shown above sequence as a squiggle, β-strands are shown as arrows labeled with β symbol and β-turns are marked by TT letters. Secondary structure assignments for all the chains is presented in Figure 1 of the SI.

promoted IR [18]. In contrast to the role of resistin in rodents, the main function of this hormone concerning obesity and IR in DMT2 is controversial in humans. Some studies have confirmed the association [19, 20], but others have challenged this link [21, 22]. A general consensus in studies with mice and humans is that resistin plays an important role in the promotion of IR, but the specific function and mechanism of resistin are still unknown (for a more extended and state-of-the-art information about RELMs function the reader is refered to the following references [13, 23–25]). Therefore, it remains the question whether or not the other members of the RELM family could share the same mechanisms and functions as resistin and an initial way to address this question is by comparing their structural features.

Resistin and RELMβ primary sequences are highly conserved, especially in the cysteine rich C terminus [1]. Human resistin is expressed mainly in leukocytes, macrophages, spleen cells and bone marrow [26, 27], whereas in rodents, it is expressed almost essentially in adipocytes [18]. RELMβ is predominantly expressed in goblet cells and epithelial cells in both humans and rodents [13]. These two RELMs are the most studied and their crystalline structures have been experimentally solved for rodents [28]. However, no exhaustive analysis and comparison of the conformation and dynamical properties have been performed for such crystal structures. One of the few studies carried out taking advantage of the crystalline structures is that of Lee and coworkers [29], in which they used the resolved structure of mouse resistin trimer to predict the pose and binding energy of CAP1-resistin model complex, leading to the experimental confirmation of a new receptor for human resistin. In another study, Surgarani and coworkers [30] modeled human resistin trimer and hexamer taking as reference mouse RELMβ, their results pointed to a chaperone-like new function of resistin. Nevertheless, the short MD simulations performed in these studies do not provide dynamic information about RELMs. A more extended simulation was performed in our previous work [31] by using mRELMβ crystal structure, however, the goal of that work was focused on the theoretical design of a set of putative ligands to target this structure and thus the protein dynamic might have been disturbed by the presence of the ligands, making the dynamic information not necessarily useful for our present purpose. Then, it is worth to perform further research on the dynamics of resistin and the dynamic differences between mouse resistin and RELMβ. An atomistic description could shed light on the biological activity and physicochemical properties of the RELMs, and support our present understanding of these hormones.

In order to have a complete outlook, we should mention that there are a few suggested RELMs receptors. ROR-1 [34] and decorin [35] are suggested receptors to mouse resistin. TLR4 [36], CAP1 [29] and human decorin [37] are suggested receptors to human resistin. In contrast, no receptors to RELMβ have been found in humans or rodents [13]. The information about binding domains in RELMs is poor as well: a study suggests that Trp82A, Trp82C, Ser64A and Ser60C are key residues in the interaction between human resistin trimer and CAP1 SH3 domain model [29]. Another experimental study suggests that TL4 receptor binds to resistin at the globular domain (amino acids 43–64 in hRes, equivalent to amino acids 27-46 in mRes) [36]. The study of such binding sites residues could serve as a reference to future studies and give insight about mechanisms of action and receptors between the different RELMs.

Regarding the dimerization process, a study suggests that Cys6 in resistin and Cys2 in RELMβ are essential for dimerization and protein stability both in mice and in humans [38]. Also, there are few studies about the effect of

temperature on the RELMs stability. In the case of human resistin, Aruna and coworkers found that it is stable to thermal denaturation below 378 K, remaining the question if it is also the case for mouse resistin homolog or other RELM members like RELMβ. Also, the research of the dynamic behavior of specific cysteine in hexameric and trimer form and their stability at high temperatures becomes very important to understand RELMs function. Aggregation phenomenon can occur too, a study suggests that by increasing the human resistin concentration the secondary structure converts from predominantly α to β conformation. It remains the question if this conformational switch could be related to functional properties as in the case of prion protein [39]. All the above questions could be better addressed if we study the dynamical characteristics of the experimental reported RELMs structures.

In this work, our objective is to characterize the dynamics of the crystallized RELMs. In order to thoroughly analyze and compare them, we perform MD simulations at 300 K and 500 K. Specifically, we evaluate the secondary structure propensity, Root-Mean-Square Deviation of Cα atoms (Cα RMSD), Solvent Accessible Surface Area (SASA) and the radius of gyration (R_g) as a function of simulation time for the following structures: murine resistin trimer (ID: 1rfx) crystal form 1, murine resistin trimer (1rgx) crystal form 2 and murine RELMβ (1rh7) trimer. Our results provide information on the structural and functional similarities of the RELMs shared between humans and rodents. This information could be useful in the search for alternative new therapeutic treatments for diabetes, inflammatory and cardiovascular diseases.

2 Methods

Each system was equilibrated by performing a MD energy minimization (EM), followed by a standard MD simulation in a canonical ensemble (MD_{NVT}) and a standard isobaric-isothermic MD simulation (MD_{NPT}). Finally, we performed Molecular Dynamics (MD) simulation (200 ns). The systems are: 1) murine resistin trimer (ID:1rfx, $C222_1$, mRes1), 2) murine resistin trimer (ID:1rgx, C2, mRes2) and 3) murine RELMβ trimer (ID:1rh7, mRELMβ-Trim). All systems were simulated at two temperatures: 300 and 500 K.

During the MD simulations, we observed the evolution on time of: Cα RMSD, secondary structure propensity, Solvent-Accesible Surface Area (SASA), gyration radio of the protein (R_g), the Root-Mean-Square Deviation (RMSD) of important residues like Trp82A, Trp82C, Ser64A and Ser60C.

3 Computational details

Missing atoms in the crystal were modeled with Swiss PdbViewer and all molecules that were not in the protein were removed. Missing residues were added with Modeller. All mRes were completed with the missing residues marked in the PDB original file (Missing residues 1-5). All calculations: EM, MD_{NVT}, MD_{NPT} and MD_{prod} were performed using GROMACS 5.1.4 with GPU support [40]. All simulations were done with molecules hydrated. We used the Amber99SB-ILDN [41] force field for the proteins in all cases.

We used TIP3P model for water molecules. The molecules were solvated in a box (x=8, y=8 and z=24 nm). Periodic boundary conditions and sodium and chloride ions were added to neutralize the system.

EM steps were carried out using the steepest descent algorithm. In NVT ensemble simulations, harmonic position restraints were applied to the solute heavy atoms with a force constant of 1000 kJ mol^{-1} nm^{-2}. The MD production runs were carried out using a time step of 2 fs. Pressure coupling uses Berendsen [42] at 1 bar. The temperature was controlled by Langevin dynamics at 300 K. A cut-off distance of 1.0 nm for Coulomb and Van der Waals neighbor list was updated according to the Verlet cut-off scheme. The long-range part of the Coulomb interactions was evaluated using PME [43] method with a relative tolerance of 10^{-5}, order 6 and Fourier spacing of 0.1. All bonds were constrained using LINCS [44], while SETTLE [45] was used for constraining the water molecules.

In clustering, we used a cut-off in root-mean-square deviations (RMSD) range of 0.18 and the gromos method [46].

It is important to note that we used as main nomenclature, the PDB numbering of mRes(1-2), residues 1 to 94 without considering the signal peptide, giving equivalences for mRELMβ when necessary. Equivalent amino acids are considered when primary sequences are aligned.

4 Results and discusion

4.1 mRes1, mRes2 and mRELMβ

First of all, we compared the MD simulation of murine resistin (1rfx, $C222_1$) trimer crystal form 1 (mRes1), murine resistin (1rgx, C2) trimer crystal form 2 (mRes2) and murine RELMβ (1rh7) trimer (mRELMβ) at room temperature.

In Figure 3a, we can observe that SASA values follow the decreasing trend mRes1 > mRes2 > mRELMβ during the simulation. Difference between mRes(1-2) and mRELMβ appears to be related with the total number of aminoacids (mRELMβ has 81 amino acids while mRes(1-2) have 94 amino acids) and hydrophilic/hidrophobic nature of aminoacids present in the protein sequences (mRes(1-2) have 54 hydrophilic amino acids and mRELMβ has 48 hydrophilic amino acids as showed in Figure 4). Difference between mRes1 and mRes2 instead, appears to be related with the compactness of the globular region in each structure. In Figure 5, it can be seen that in the superimposed crystal structures, mRes1 has slightly more open conformation than mRes2. Figure 6 shows that mRes1 is more open (less compact) in the head domain than mRes2 and mRELMβ during the simulation at 300 K, as also suggested by Patel and coworkers [28].

In terms of intramolecular interactions, we can see in Figure 3b that mRELMβ form less H_{bonds} than mRes(1-2), and mRes1 less than mRes2. Furthermore, Table 1 presents the main interchain H_{bonds} that stay conserved during the major part of the simulations (90% of the time). We identified a distinctive frequent interaction network that is common in mRes(1-2) and mRELMβ, which is formed between Arg86A-Val147B (Arg76A-Val124B in mRELMβ), Arg180B-Val241C (Arg157B-Val205C in mRELMβ) and, Arg274C-Val53A (Arg248C-Val43A in mRELMβ), this means the interaction network is symetric, as can be seen in Figure 7. We also identified a frequent interaction network in mRELMβ that is absent in mRes(1-2), this is formed between Thr44A-Thr125B-Thr206C (there are no such equivalent amino acid in mRes(1-2)). Therefore, we postulate that the former interactions networks might be responsible for the interchain stability in the globular region of mRes(1-2) and mRELMβ.

Fluctuations of R_g values give an idea of the conformational movements of the whole protein and R_g values of protein compactness. R_g is presented in Figure 3c, where we can see that R_g values for mRELMβ are lower than those for mRes(1-2), and values for mRes2 are lower than those for mRes1. The R_g average values in the last 100 ns of simulation are 2.23, 2.31 and 2.35 nm for mRELMβ, mRes1 and mRes2, respectively.

Since we wanted to compare properties of important residues involved in RELMs interactions with putative receptors, we monitored SASA values of Trp82A and Trp82C as mentioned before [29]. In Figure 3d-e we can see that Trp82A and Trp82C conserve similar SASA during the entire simulation, showing similar exposition to water in the three systems. The mRes1 shows a slightly more SASA than mRes2 and mRELMβ, in part due to the different orientation with respect to water of Trp amino acid on the different proteins during simulations. About the orientation, mRes1 has a $\chi 1$ preference dihedral angle of -70^o which points upwardas in a more water exposed orientation, as shown in Figure 8; mRes2 and mRELMβ instead, point downwards during all the simulation, in a less water exposed mode. There seems to be a high energy barrier between the Trp82A states in the two crystal structures reported in the PDB (mRes1 and mRes2). This last result shows us that special care must be taken when modeling human resistin by using mRes1, mRes2 or mRELMβ as template. Even the same protein (mRes) but taking different structures (mRes(1-2)) could lead to different sidechain conformations apparently separated by high energy barriers as in the case of Trp82A and then it is unlikely that the same receptor interactions can occur.

Even if the three systems show similar SASA in some amino acids, the average environment around these amino acids could be dissimilar, for instance, in Figure 9, the environment around Trp82A in mRes1 is slightly hydrophilic meanwhile in mRELMβ it is mostly hydrophobic. The estimated hydrophilic environment of Trp82 is in agreement with

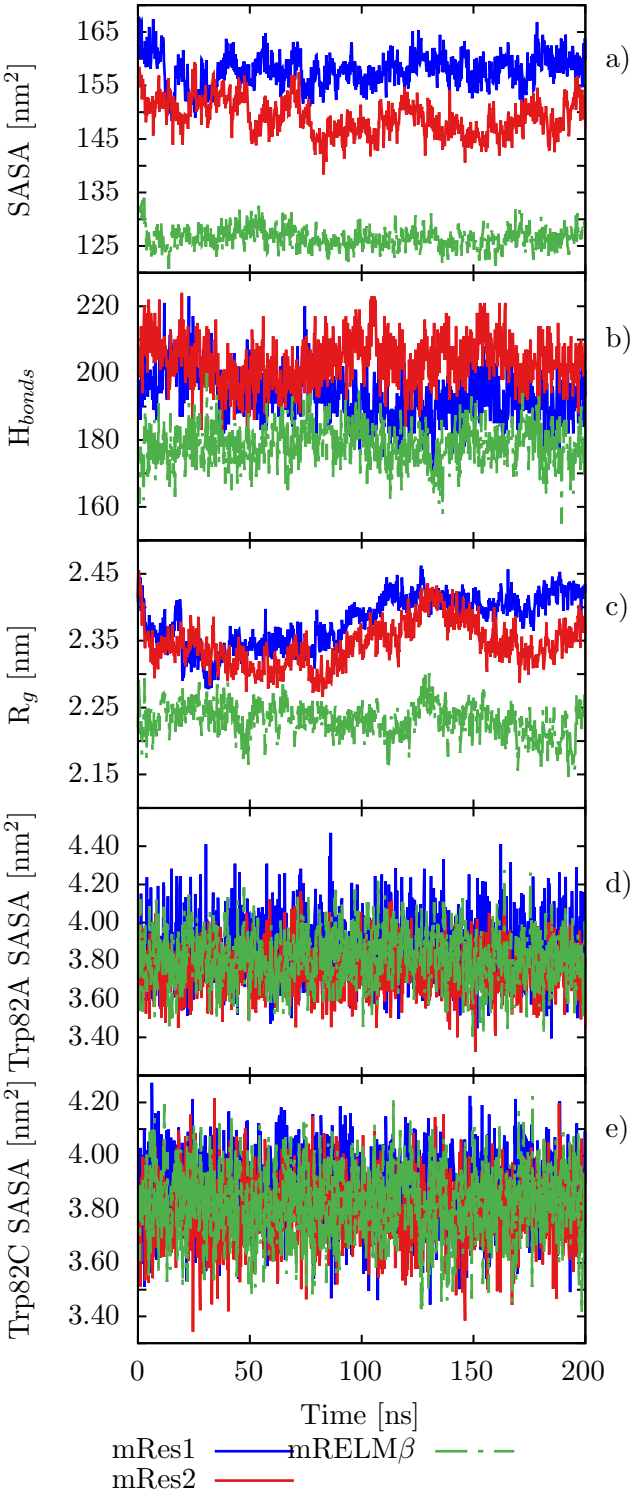

Figure 3: Structural changes for mRes1, mRes2, and mRELMβ. Time evolution of a) protein SASA, b) intraprotein H_{bonds}, c) protein gyration radio, d) Trp82A SASA and e) Trp82C SASA. T= $300K$. Trimer form.

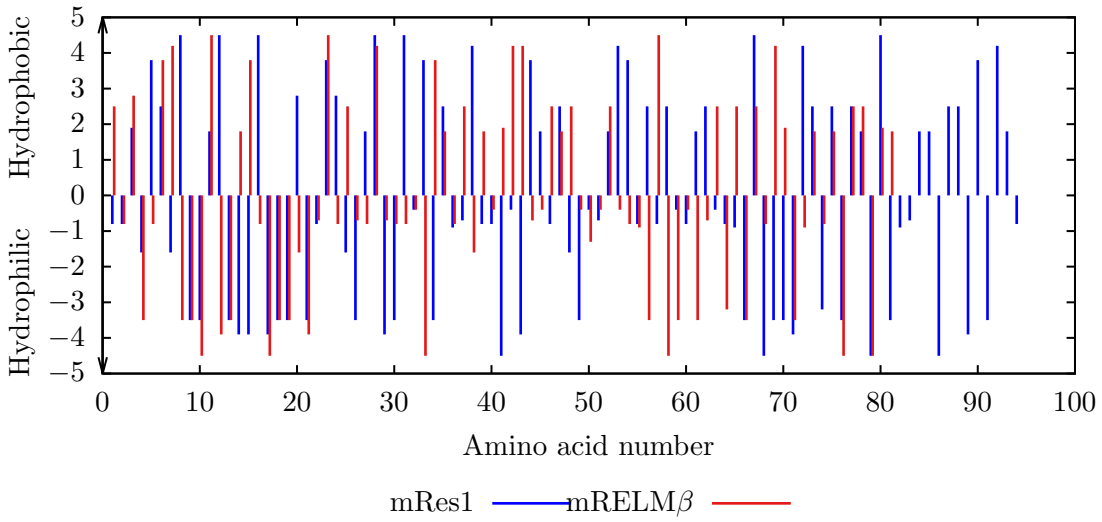

Figure 4: Classic Kyte & Doolittle hydropathy plot [47] of mRes1 and mRELMβ proteins. mRes1 has 54 hydrophilic amino acids and mRELMβ has 48 hydrophilic amino acids. Window = 1.

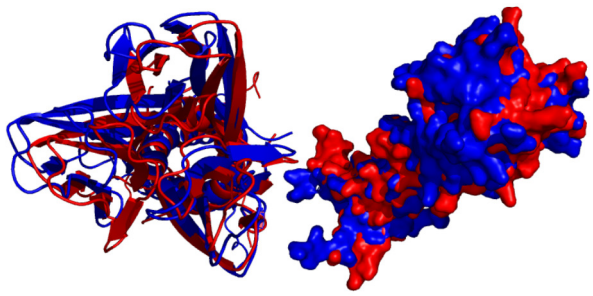

Figure 5: Murine resistin (1rfx,C222$_1$) trimer crystal form 1 (mRes1) and murine resistin (1rgx,C2) trimer crystal form 2 (mRes2) superimposed structures. mRes1 is colored in blue and mRes2 in red.

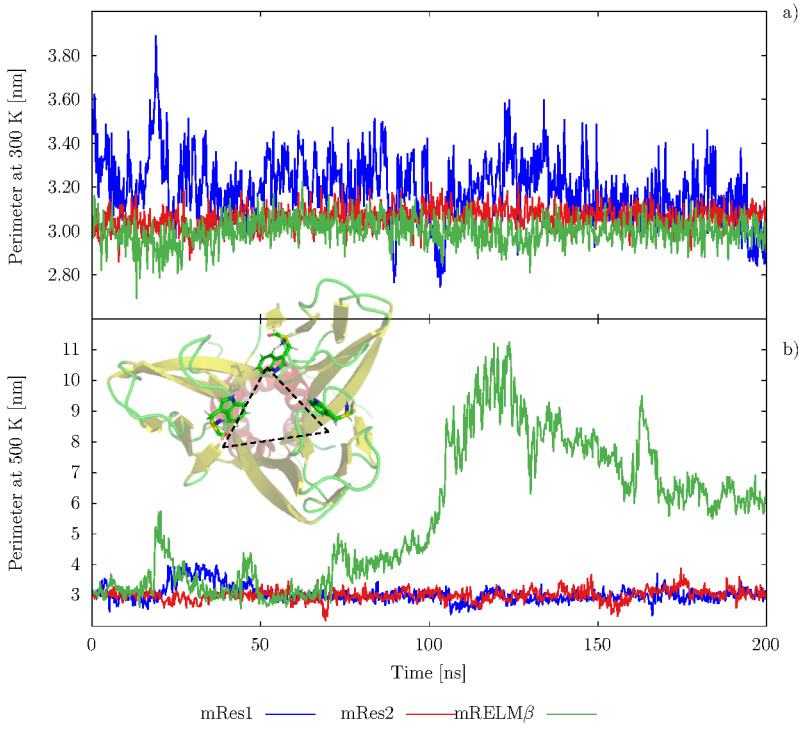

Figure 6: The perimeter of the triangle formed by 3 Trp amino acids (amino acids 65, 159 and 263 in mRes(1-2) and amino acids 55, 136 and 217 in mRELMβ) in the globular part of proteins as shown in the figure inset. a) simulations at 300 K and b) simulations at 500 K.

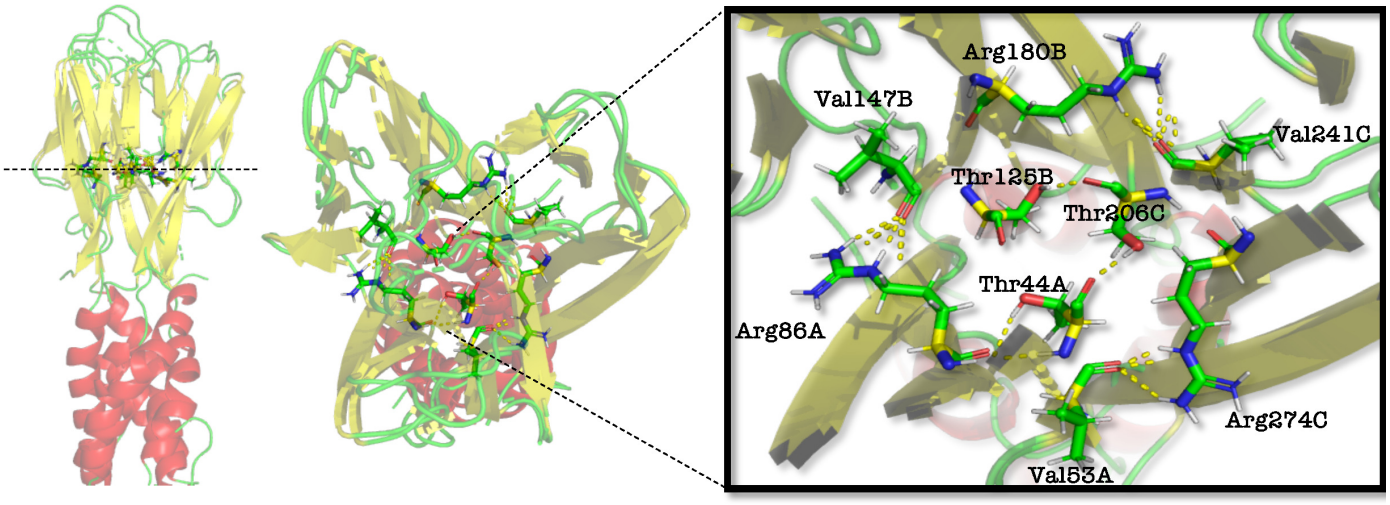

Figure 7: Residues in globular area of mRes2 and mRELMβ superimposed structures showing an important network of frequently formed interchain H_{bonds}. External network is formed in mRes(1-2) as well as in mRELMβ, internal network is only possible in mRELMβ due to the fact that Thr44 is missing in mRes(1-2) structures and instead, there is a Lys amino acid.

Table 1: Interchain hydrogen bond occupancy for mRes1, mRes2 and mRELMβ during the simulation time. Only occupancies above 90% are shown.

Chains	Donor	Acceptor	Occupancy (%)
mRes1			
A-B	Arg86-Side-NH2	Val147-Main-O	90.12
B-C	Ser252-Side-OG	Cys152-Main-O	99.30
B-C	Arg180-Side-NE	Val241-Main-O	98.30
B-C	Ser252-Side-OG	Cys152-Main-C	97.41
B-C	Arg180-Side-NH2	Val241-Main-O	95.91
B-C	Cys152-Main-N	Gly251-Main-O	92.51
B-C	Trp176-Side-CZ2	Gln264-Side-OE1	81.24
A-C	Arg274-Side-NE	Val53-Main-O	99.60
mRes2			
A-B	Ser158-Side-OG	Cys58-Main-O	100.00
A-B	Ser158-Side-OG	Cys58-Main-C	98.70
A-B	Trp159-Main-N	Ser57-Side-OG	98.00
A-B	Gly157-Main-N	Ala61-Main-O	96.41
A-B	Arg86-Side-NE	Val147-Main-O	90.02
B-C	Ser252-Side-OG	Cys152-Main-O	100.00
B-C	Arg180-Side-NE	Val241-Main-O	99.40
B-C	Ser252-Side-OG	Cys152-Main-C	98.20
B-C	Trp253-Main-N	Ser151-Side-OG	97.60
B-C	Arg180-Side-NH2	Val241-Main-O	96.71
A-C	Ser64-Side-OG	Cys246-Main-O	99.50
A-C	Arg274-Side-NE	Val53-Main-O	99.20
A-C	Trp65-Main-N	Ser245-Side-OG	99.10
A-C	Ser64-Side-OG	Cys246-Main-C	96.61
A-C	Arg274-Side-NH2	Val53-Main-O	93.91
A-C	Ser245-Side-CB	Trp65-Side-CE2	90.32
mRELMβ			
A-B	Arg76-Side-NE	Val124-Main-O	100.00
A-B	Ser135-Side-OG	Cys48-Main-O	99.70
A-B	Ser135-Side-OG	Cys48-Main-C	98.71
B-C	Arg157-Side-NE	Val205-Main-O	100.00
B-C	Ser216-Side-OG	Cys129-Main-O	95.52
B-C	Thr125-Side-OG1	Thr206-Main-O	93.53
B-C	Gly215-Main-N	Gly132-Main-O	93.13
B-C	Arg157-Side-NH2	Val205-Main-O	92.33
B-C	Ser216-Side-OG	Cys129-Main-C	92.13
A-C	Arg238-Side-NE	Val43-Main-O	100.00
A-C	Thr206-Side-OG1	Thr44-Main-O	98.80
A-C	Ser54-Side-OG	Cys210-Main-O	95.72
A-C	Thr206-Side-OG1	Thr44-Main-C	95.12
A-C	Cys210-Main-N	Gly53-Main-O	95.12
A-C	Gly53-Main-N	Gly213-Main-O	93.82
A-C	Arg238-Side-NH2	VAal43-Main-O	93.43
A-C	Ser54-Side-OG	Cys210-Main-C	92.03
A-C	Gly53-Main-N	Gly213-Main-C	91.63

the experimentally reported partially polar environment of this same tryptophan in recombinant hRes [39]. In the case of Ser60 and Ser64 we can observe a similar trend for all proteins (except for mRELMβ laking Ser60 amino acid). Regarding the segment between 27 and 46 amino acids, we can observe that hRes and mRes show a similar trend, meanwhile

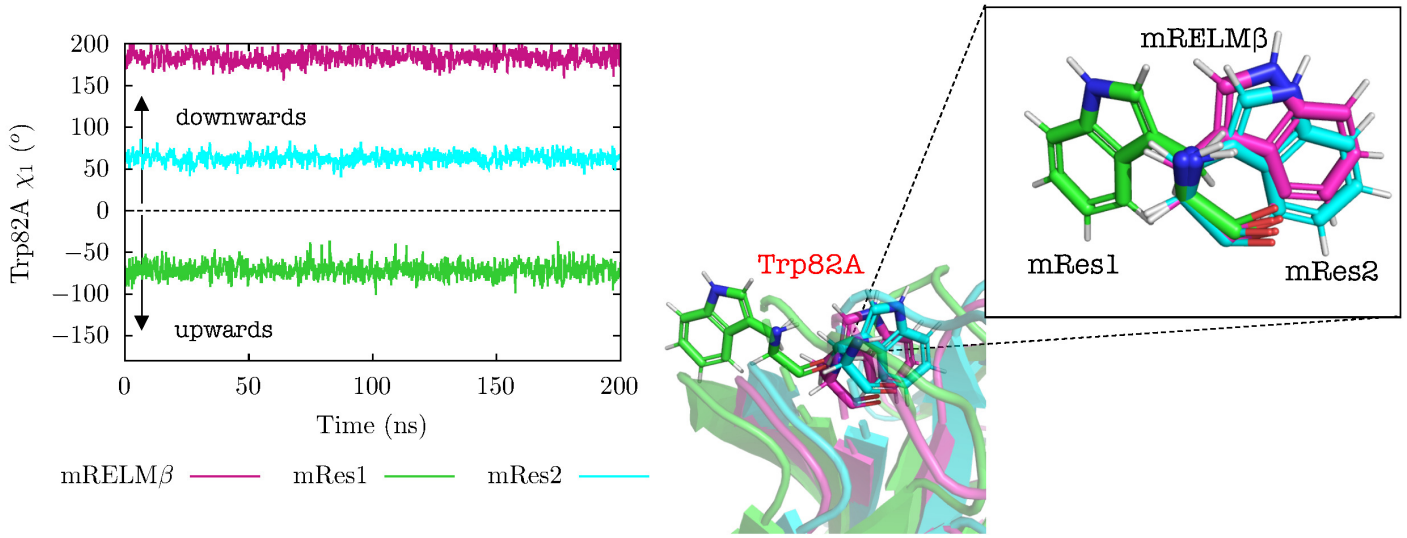

Figure 8: Trp82A on mRes1(green), mRes2(blue) and mRELMβ(pink).

mRELMβ does not have an equivalent first half part of the segment and present a different environment pattern in the second half part of the segment, being mostly hydrophobic compared to the hydrophilic environment of mRes1 and hRes.

We can observe in Figure 10a that mRes1, mRes2 and RELMβ have a similar percentage of structured amino acids and in Figure 10b that RELMβ has slightly more percentage of coiled amino acids as a result of an extended nonhelical neck region non present in mRes(1-2) [28]. In Figure 10c-d, it can be seen that RELMβ has slightly more content of β-Sheet and less content of α-Helix than mRes(1-2), the latter in agreement with a shorter coiled-coil region, comprising only four turns of helix from each protomer, compared with the six turns in mRes(1-2) [28]. It was confirmed the predominantly β-sheet structure of mRes, in contrast with the reported majority content of α-helices in hRes [26,39]. In the case of recombinant mRes there is also a report [48] that suggests a majority of α-helix structure content, so it remains controversial. We can observe a loss in α-Helix content in both mRes during the first 50 ns of simulation, probably due to the effect of the unstructured 6 amino acids in the tail.

Secondary structure maps in Figure 11a show that in mRELMβ, α-helices are prone to convert into a turn or 3-Helix through the simulation, being chain B the chain most importantly affected. In general, it can be seen a more disordered region between α-Helix and the first β-Sheet in this protein compared with mRes(1-2). In the case of mRes1 in Figure 11b, the α-helices are prone to convert into a turn, bend or 3-Helix through the simulation, being chain A the most importantly affected. In more detail, chain A losses α-helix structure after 30 ns between amino acids 10 and 20, chain B after 20 ns around amino acid 120, chain C after 15 ns around amino acid 215 and chain C after 180 ns around amino acid 200. This protein has a 3-Helix structure between α-Helix and the first β-Sheet, mostly in chain A. We can observe that the third β-Sheet of chain B (around amino acid 150) tends to be lost during an extended part of the simulation. In the case of mRes2 in Figure 11c, the α-helices are prone to convert into a turn, bend, 3-Helix or 5-Helix through the simulation, being chain B the most importantly affected. In more detail, chain A losses α-helix structure after 5 ns between amino acids 20 and 30, and chain B after 30 ns between amino acids 110 and 130. This protein also has a 3-Helix structure between α-Helix and the first β-Sheet in all chains. We can observe that the third β-Sheet of chain B (around amino acid 150) tends to be lost.

Figure 12a shows that the RMSD of Cα is more stable for mRes1 and mRELMβ than for mRes2. This could imply that mRes1 and mRELMβ adopt more similar conformations over the dynamics, while mRes2 visits a second important conformation different from the initial one (details of RMSD distributions in Figure 13) or that mRes2 has a longer equilibration period. In order to detect the protein segments with important position fluctuations, the Root mean square fluctuations (RMSF) of all protein atoms was measured and presented in Figure 14a-b, showing the expected high fluctuation around the beginning and end of each chain and also high RMSF values after the fifth β-strand (amino acid 76 of each chain) in mRes1 and mRes2; for mRELMβ, on the other hand, besides the beginning and end of the chains, high

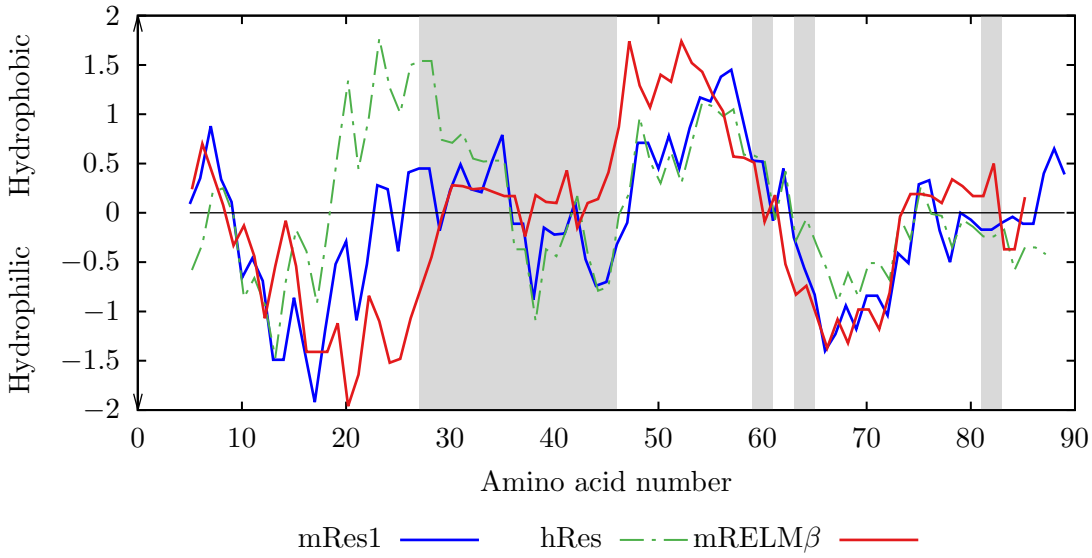

Figure 9: Classic Kyte & Doolittle hydropathy plot of mRes1, hRes and mRELMβ proteins [47]. The residues involved in interactions with putative receptors reported in the literature are in shadows [29,36]. In order to present aligned sequences of the structures, glycine was used instead of insertions at the beginning of the sequence of RELMβ.

RMSF fluctuations were found in the α-helical region (first 20 amino acids of each chain). Trp82A has from mRes2 and mRELMβ has similar RMSD in mRes2 and mRELMβ but in mRes1 it has a broader range of RMSD values, as shown in Figure 12b. Trp82C has similar behavior in the three systems, as shown in Figure 12c. Ser64A in mRes2 and mRELMβ has a similar pattern of RMSD values in mRes1 and mRes2 as shown in Figure 12e, while in mRes1 it seems to adopt a second most visited conformation, as shown in Figure 12d. Ser60 has a similar pattern In Figure 12e, while mRELMβ does not have an equivalent residue in its sequence. We speculate that mRes2 and mRELMβ have higher probability of having similar environment and sharing interactions mechanisms that includes Trp82A and Ser64A.

4.2 mRes1 at 300 and 500 K

We analize and compare the conformational space of murine resistin (1rfx,C222$_1$) trimer crystal form 1 (mRes1) at 300 and 500 K.

In Figure 15a we can observe that mRes1 tends to lose SASA at high temperature after 100 ns. According to Figure 15b, mRes1 at 300 K form less H_{bonds} than at 500 K after 100 ns. Here we checked the Hbond network persistence at elevated temperature, we observed a reduced occupancy in Hbonds formed between Arg86A-Val147B, Arg180B-Val241C and, Arg274C-Val53A for mRes1, going between 56% and 73% of occupancy, giving rise to a new important interaction between Arg274C and Glu70A and the equivalent residues in the other chains. R_g is showed in Figure 15c, it increases in mRes1 at 500 K. Finally in Figure 15d-e we can see that Trp82A and Trp82C conserve similar SASA during the entire simulation, showing slightly less exposition to water at 500 K.

We can observe in Figure 16 that mRes1 at 500 K has less percentage of structure than at 300 K, and more percentage of coil content. Content of β-Sheet is less in mRes1 at 500 K in the first half of simulation, but in the second half they have similar content. We can observe a loss in α-Helix content in mRes1 at 500 K.

In Figure 17 we can observe that the RMSD of Cα in mRes1 at 300 K is smaller than at 500 K. At 300 K the simulation converge from the first nanoseconds, while at 500 K until after the first half of the simulation. RMSD of Cα in mRes1 at 300 K is around 0.4 nm. RMSD of Cα in mRes1 at 500 K is around 2 nm. Trp82A RMSD at 500 K has values around

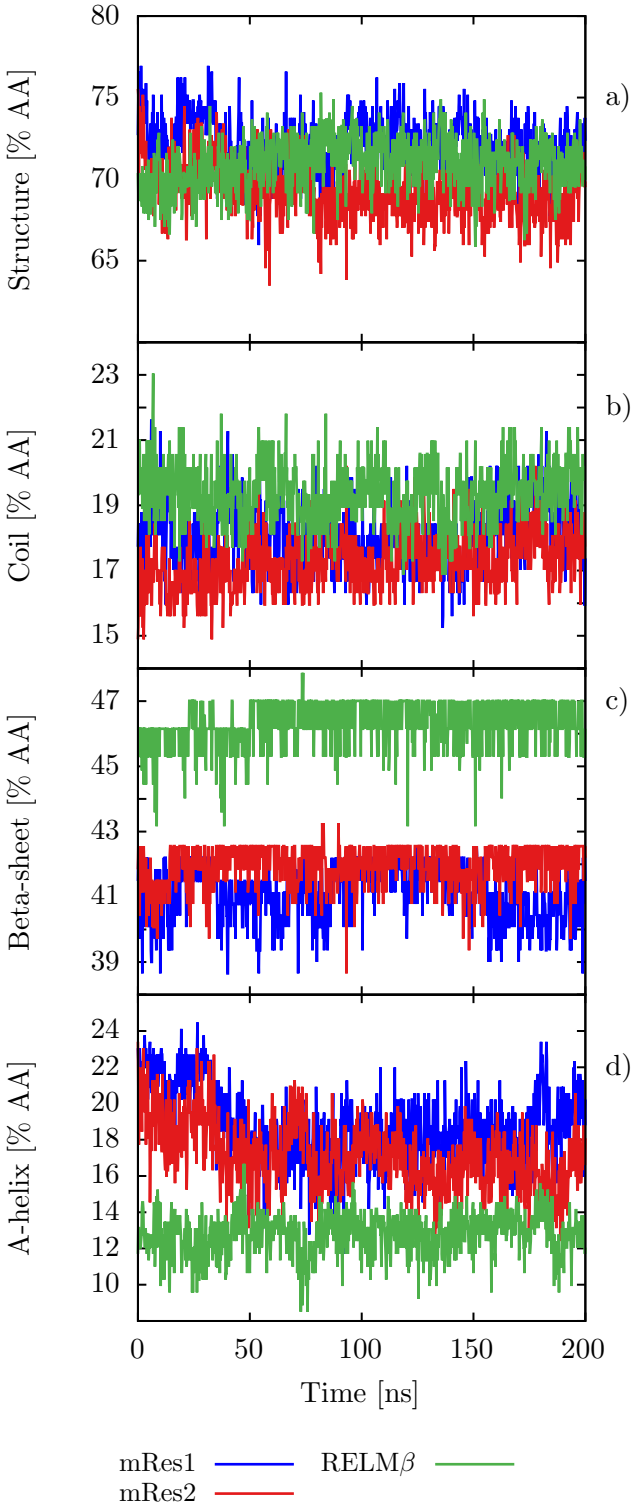

Figure 10: Secondary structure content of mRes(1-2) and mRELMβ. a) Protein Structure = α-Helix + β-Sheet + β-Bridge + Turn, b) Coil, c) β-Sheet, d) α-Helix. T= $300K$. Trimer form. AA states for amino acid.

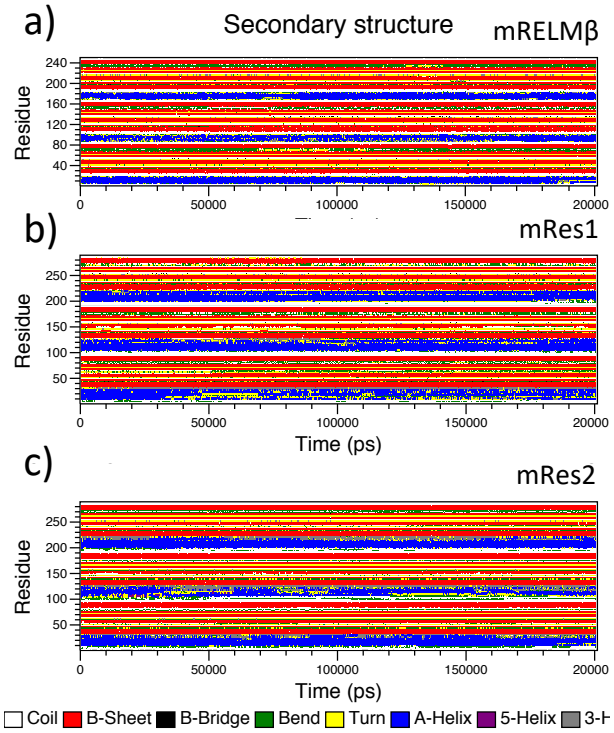

Figure 11: Secondary structural fluctuations of a) mRELMβ, b) mRes1 and c) mRes2. T= 300K. Trimer form.

0.14 ns in conjunction with shorter periods of values around 0.02 nm. Trp82A RMSD at 300 K has values around 0.02 nm during the entire simulation. Trp82C RMSD at 500 K shows similar behaviour. Ser64A RMSD at 300 and 500 K shows a dual behaviour around 0.02 and 0.07 nm. Ser60C RMSD at 300 and 500 K has values around 0.03 nm in conjunction with shorter periods of values around 0.07 nm.

The time course evolution of the secondary structure at two temperatures is shown in Figure 18. At 300 K the protein retains its secondary structure. At 500 K the protein loses great part of its A-helix structure, which tends to convert into a turn or β-Sheet form.

At 500 K, mRes1 loses most of their secondary structure as can be seen in Figure 19. In general, we can observe that the simulation reaches equilibrium after the first 100 ns. The first zone to lose its structure is the α-helical tail segment. There is a helical part particularly stable around amino acids 15-17 in chain A. There are two segments that originally form part of the helical part that convert into β-sheet around 91-93 and 201-206 of chain A and C, respectively.

4.3 mRes2 at 300 and 500 K

We analize and compare the conformational space of murine resistin (1rgx) trimer crystal form 2 (mRes2) at 300 and 500 K.

In Figure 20 we can observe that mRes2 tends to mantain SASA at high temperature during simulations. mRes2 at 500 K form less H_{bonds} than at 300 K during the whole simulations. Here we checked the Hbond network persistence at elevated temperature, we observed a reduced occupancy in Hbonds formed between Arg86A-Val147B, Arg180B-Val241C and, Arg274C-Val53A in mRes2, going between 23% and 80% of occupancy, giving rise to a new important interaction between Arg274C and Glu70A and the equivalent residues in the other chains. R_g decreases in mRes2 at 500 K. Trp82A and Trp82C conserve similar SASA during the entire simulation.

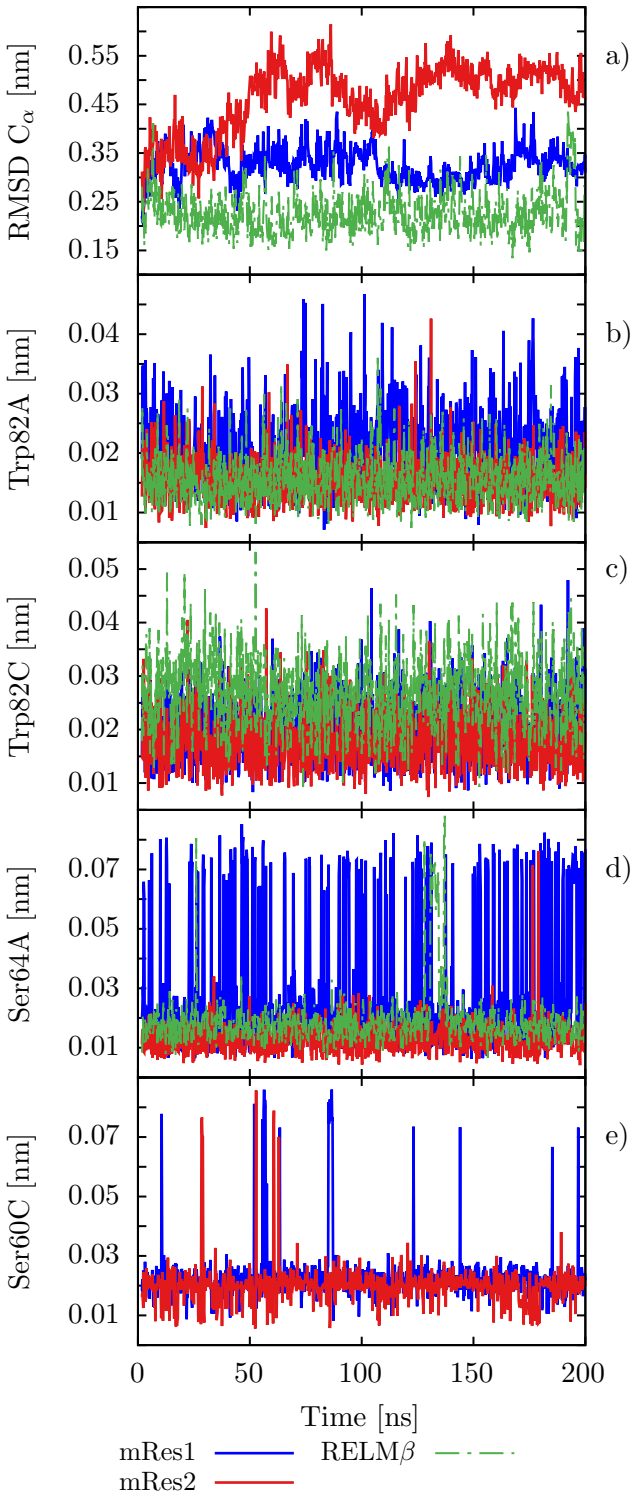

Figure 12: Proteins RMSD of a) Cα, b) Trp82A, c) Trp82C, d) Ser64A and e) Ser60C. T= 300K. Trimer form.

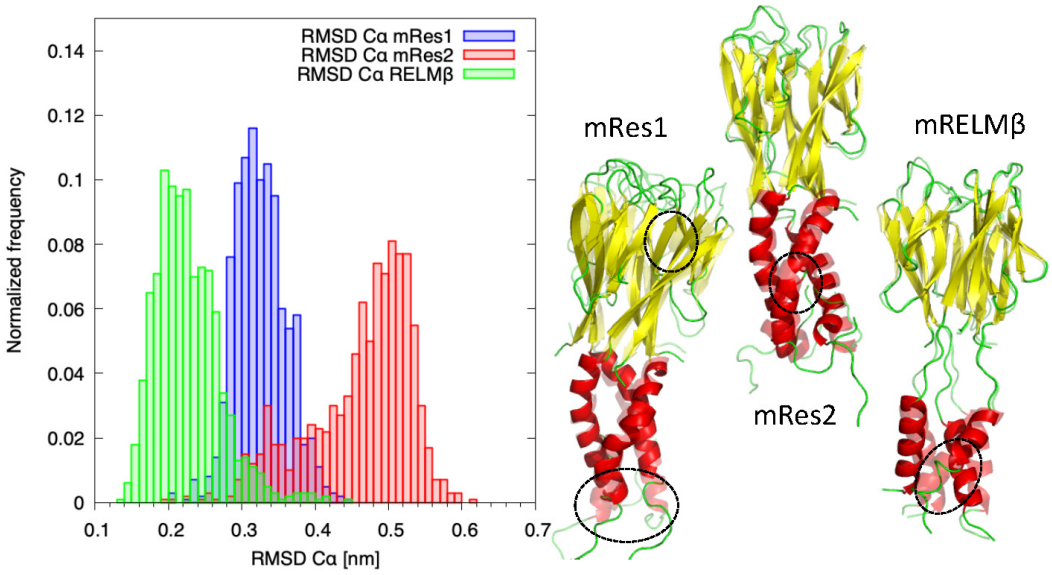

Figure 13: RMSD distribution of Cα in the different proteins and a representative structure of each distribution. T= 300K. Trimer form.

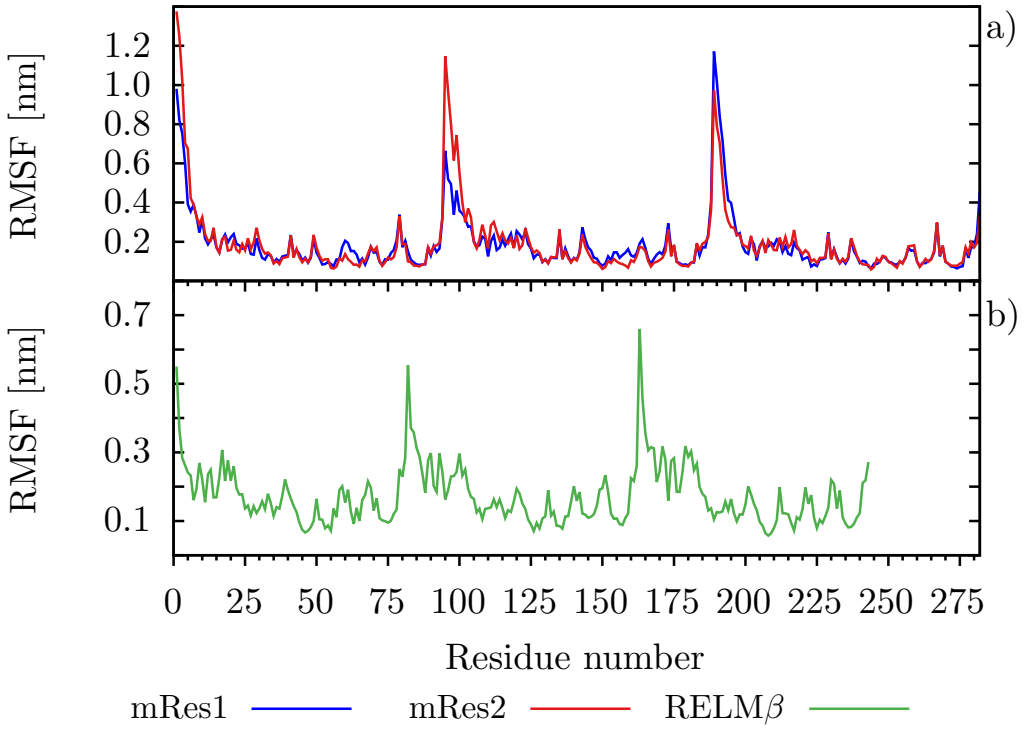

Figure 14: RMSF of heavy atoms of a) mRes(1-2) and b) mRELMβ. T= 300K. Trimer form.

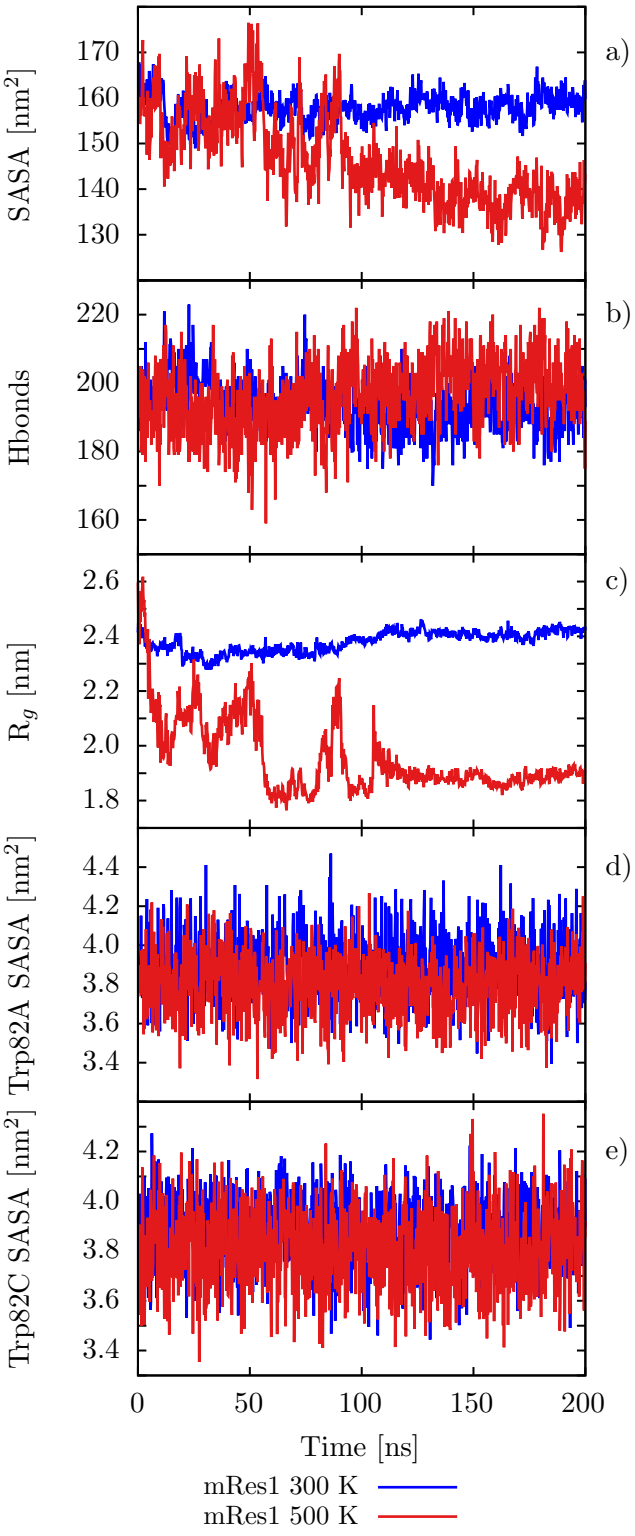

Figure 15: mRes1 characteristics at two temperatures. a) Protein SASA, b) H_{bonds}, c) protein compactness, d) Trp82A SASA and e) Trp82C and SASA. Trimer form.

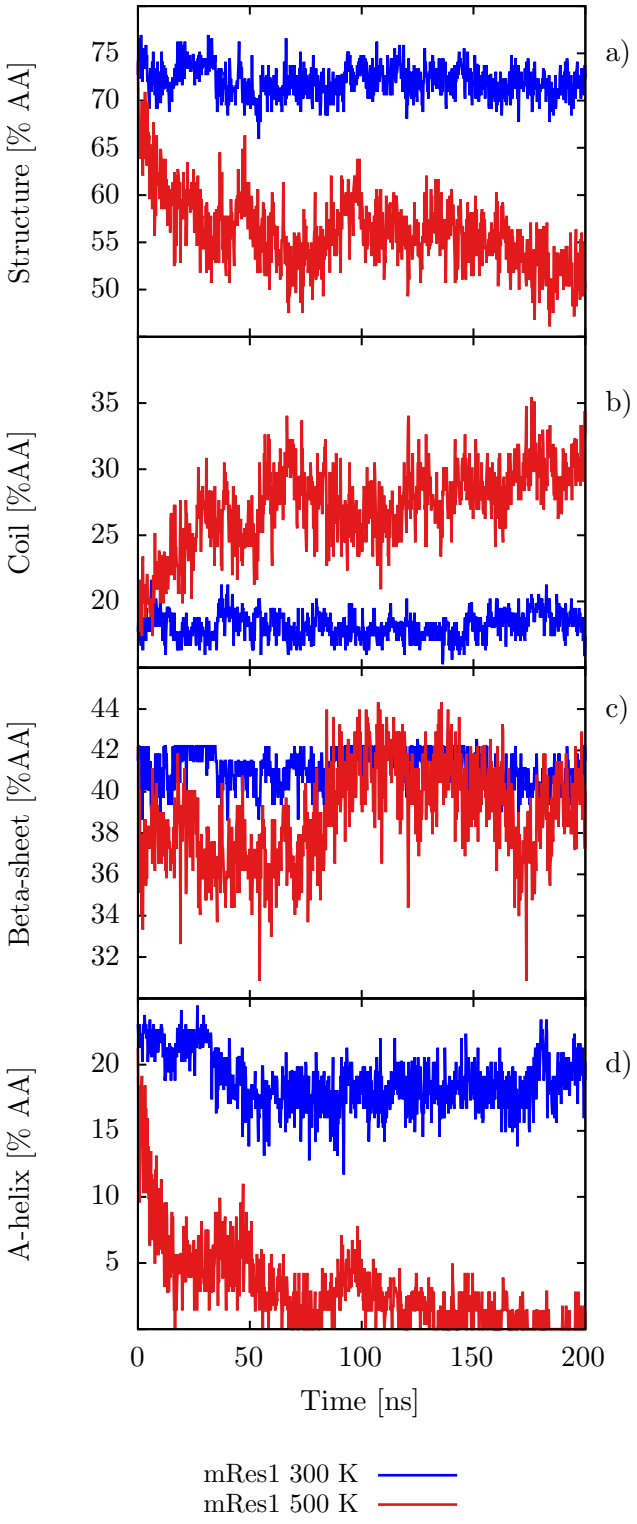

Figure 16: mRes1 at two temperatures. a) Protein Structure = α-Helix + β-Sheet + β-Bridge + Turn, b) Coil, c) β-Sheet, d) α-Helix. T= $300K$. Trimer form. Here, AA means amino acid.

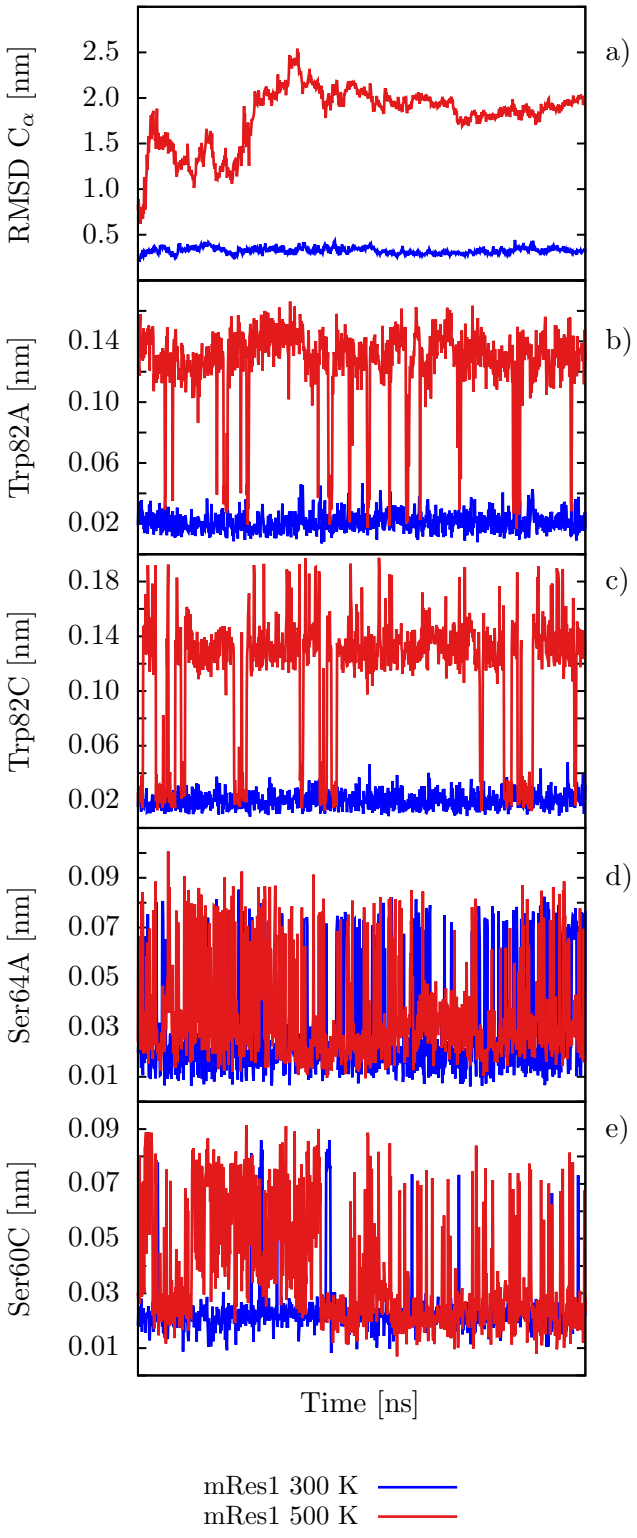

Figure 17: mRes1 at two temperatures. a) RMSD of Cα, b) Trp82A, c) Trp82C, d) Ser64A and e) Ser60C. T= 300K. Trimer form.

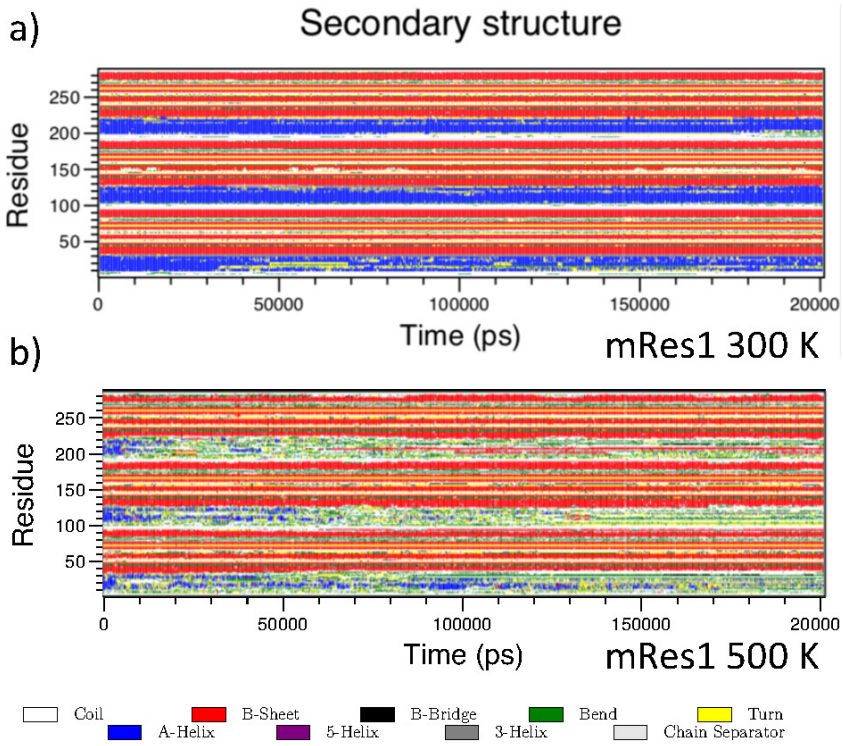

Figure 18: Secondary structural fluctuations of mRes1 at a) 300 K and b) 500 K. Trimer form.

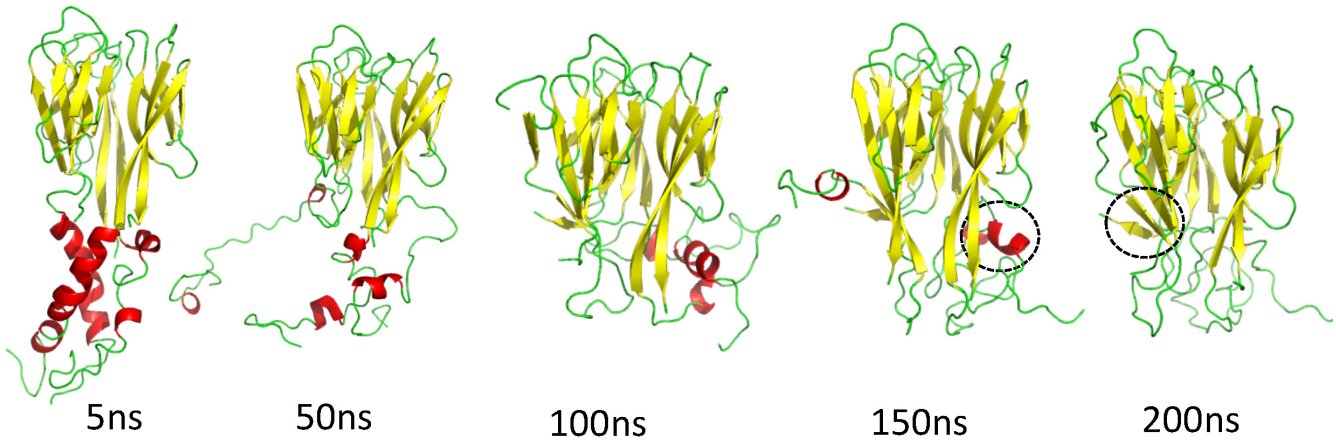

Figure 19: Snapshots every 50 ns of the simulation at 500 K for mRes1.

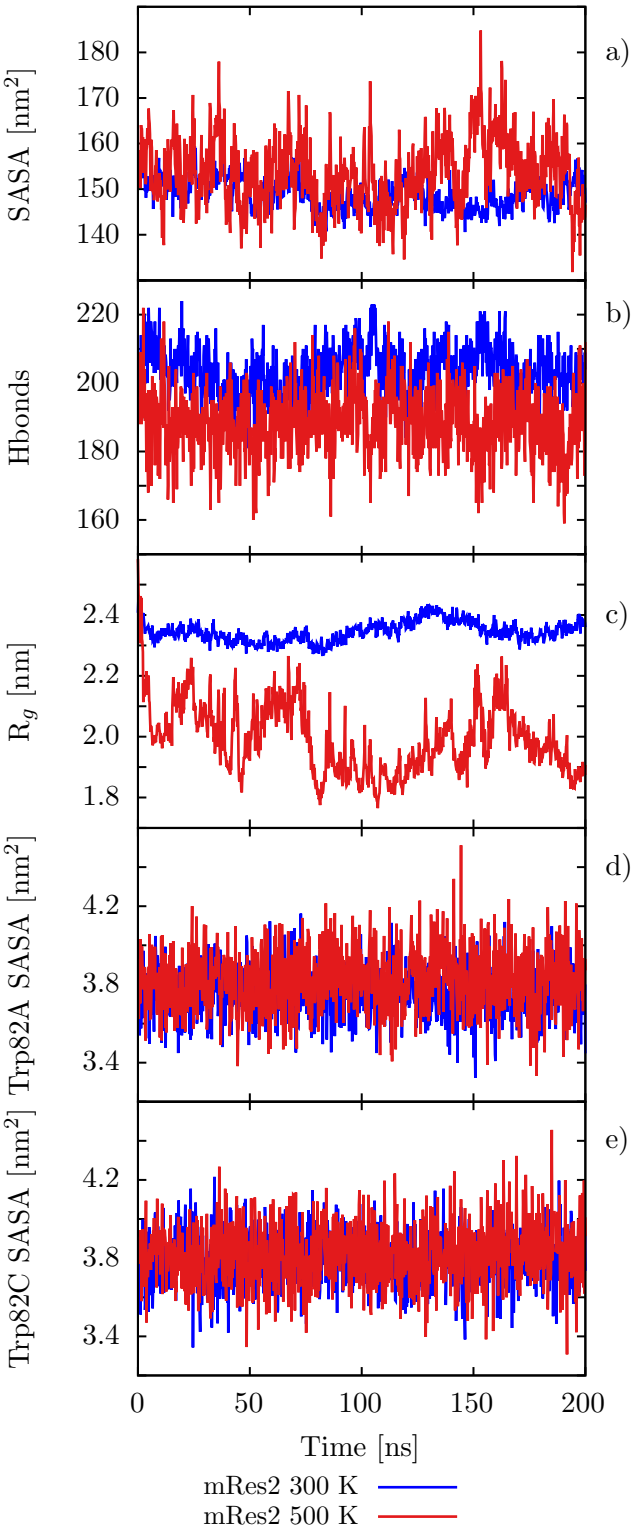

Figure 20: mRes2 characteristics at two temperatures. a) Protein SASA, b) H_{bonds}, c) protein compactness, d) Trp82A SASA and e) Trp82C and SASA. Trimer form.

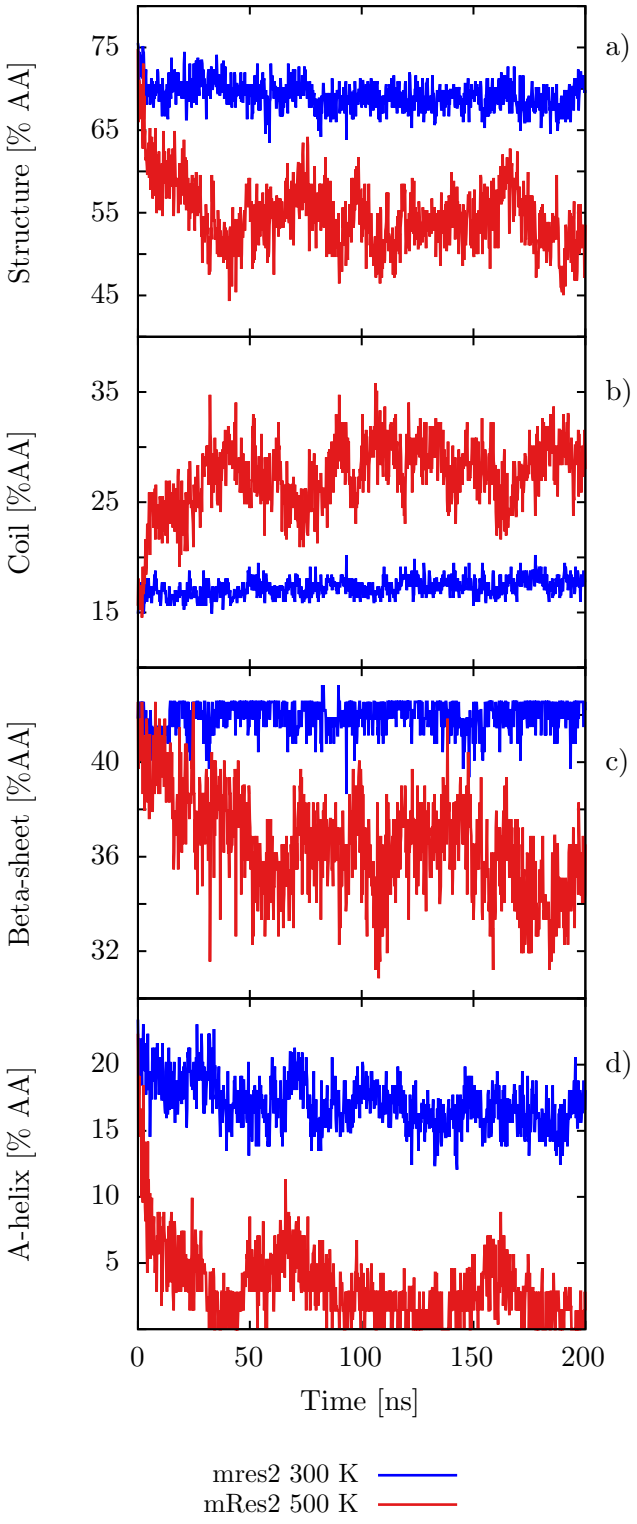

Figure 21: mRes2 at two temperatures. a) Protein Structure = α-Helix + β-Sheet + β-Bridge + Turn, b) Coil, c) β-Sheet, d) α-Helix. T= $300K$. Trimer form. Here, AA means amino acid.

We can observe in Figure 22 that mRes2 at 500 K has less percentage of structure than at 300 K, and more percentage of coil content. Content of β-Sheet is less in mRes2 at 500 K from the first nanoseconds of the simulation. We can observe a lost in α-Helix content in mRes2 at 500 K.

RMSD of Cα in mRes2 at 300 K is smaller than at 500 K: RMSD of Cα in mRes2 at 300 K is around 0.5 nm. RMSD of Cα of mRes2 at 500 K is around 1.5 nm. Trp82A RMSD at 500 K has values around 0.14 ns in conjunction with shorter periods of values around 0.02 ns. Trp82A RMSD at 300 K has values around 0.02 during the entire simulation. Trp82C RMSD at 500 K has similar behaviour. Ser64A RMSD at 300 shows a behaviour around 0.02 and a dual behaviour at 500K around 0.02 and 0.07 nm. Ser60C RMSD at 500 K has values around 0.02 nm in conjunction with periods of values around 0.07 nm, meanwhile at 300 K the RMSD value is around 0.02 nm.

The time course evolution of the secondary structure at two different temperatures of mRes2 is shown in Figure 23. At 300 K the protein retains its secondary structure. At 500 K the protein loses great part of its α-helix structure, which tends to convert into a turn or β-Sheet form.

At 500 K, mRes2 loses most of their secondary structure as can be seen in Figure 24. In general, we can observe that the simulation reaches equilibrium after the first 50 ns of simulation. The first zone to lose its structure is the α-helical tail segment. There is a helical part particularly stable around amino acids 100-106/114-116 in chain A and 207-211 in chain C. There are two segments that originally form part of the helical part that convert into β-sheet around 26-29 in chain A.

4.4 mRELMβ at 300 and 500 K

We analize and compare the conformational space of murine RELMβ (1rh7) trimer at 300 and 500 K.

In Figure 25 we can observe that mRELMβ tends to mantain SASA fluctuation between 120 and 150 nm^2 during simulations at high temperature. mRELMβ at 500 K forms similar number of H_{bonds} than those at 300 K during the whole simulations. Here we checked the Hbond network persistence at elevated temperature, we observed a strongly reduced occupancy in Hbonds formed between Arg76A-Val124B, Arg157B-Val205C and, Arg248C-Val43A for mRELMβ, going between 6% and 16% of occupancy. R_g decreases in mRELMβ at 500 K. Trp82A and Trp82C conserve similar SASA during the entire simulation.

We can observe in Figure 27 that mRELMβ at 500 K has less percentage of structure than at 300 K, and more percentage of coil content. Content of β-Sheet is less in mRELMβ at 500 K since the first nanoseconds of the simulation, eventually at the end of the simulation it returns to a similar content of β-Sheet. We can observe a lost in α-Helix content at 500 K.

RMSD of Cα in β-Sheet at 300 K is smaller than at 500 K: RMSD of Cα in β-Sheet at 300 K is around 0.3 nm. RMSD of Cα of mRes2 at 500 K is around 2 nm. Trp82A RMSD at 500 K has values around 0.14 ns in conjunction with shorter periods of values around 0.02 ns. Trp82A RMSD at 300 K has values around 0.02 during the entire simulation. Trp82C RMSD at 500 K shows similar behaviour. Ser64A RMSD at 300 K shows a behaviour around 0.02 and a dual behaviour at 500 K around 0.02 and 0.08 nm. Ser60A RMSD at 500 K has values around 0.03 nm in conjunction with periods of values around 0.14 nm, meanwhile at 300 K the RMSD value is around 0.03 nm and sometimes around 0.12 nm.

The time course evolution of the secondary structure of mRELMβ at two different temperatures is shown in Figure 28. At 300 K the protein retains its secondary structure. At 500 K the protein loses great part of its α-helix structure, which tends to convert into a turn, coil or β-Sheet form.

At 500 K, mRELMβ loses most of their secondary structure as can be seen in Figure 29. In general, we can observe that the simulation reaches equilibrium after the first 100 ns of simulation. The first zone to lose its structure is the α-helical tail segment but rapidly also the three stranded β-sheet jelly roll structure is being afected as also shown in Figure 6b, finally the three chains separate from each other. There is a helical part particularly stable around amino acids 21-24/174-180 in chains A and C, respectively.

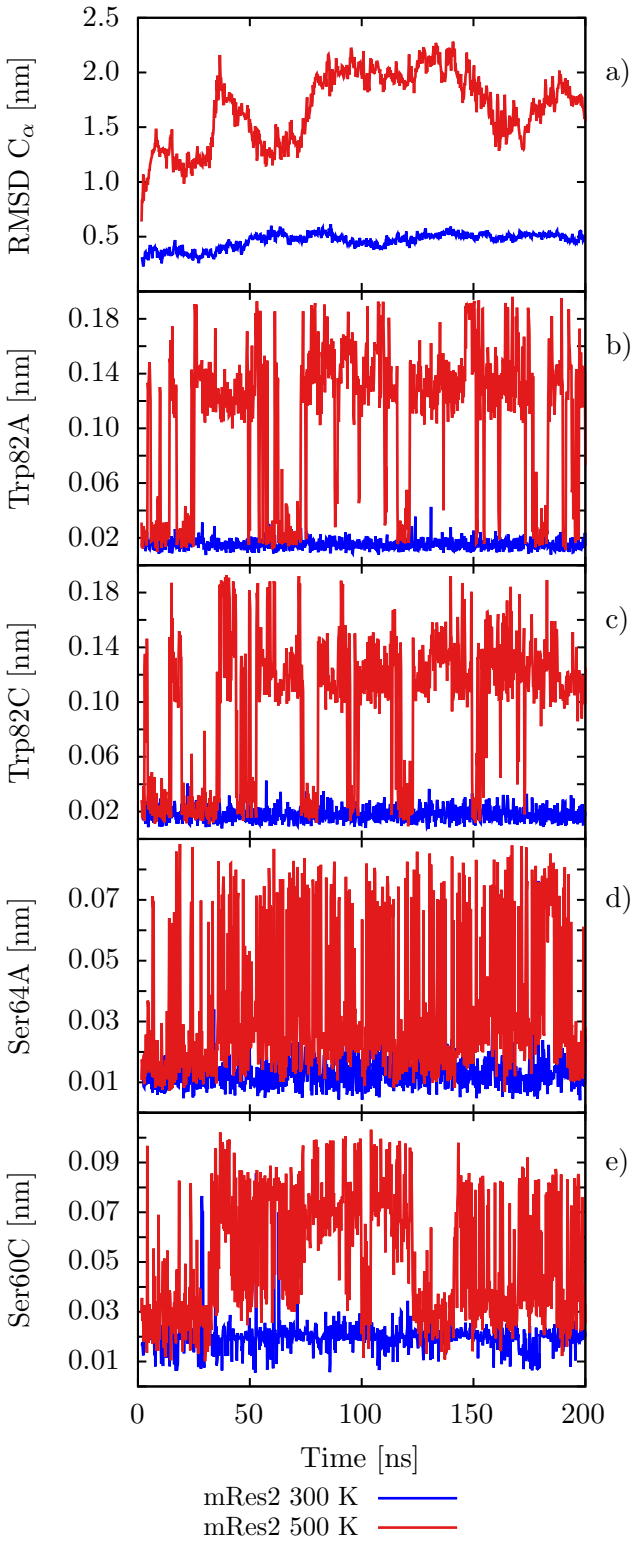

Figure 22: mRes2 at two temperatures. a) RMSD of Cα, b) Trp82A, c) Trp82C, d) Ser64A and e) Ser60C. T= 300K. Trimer form.

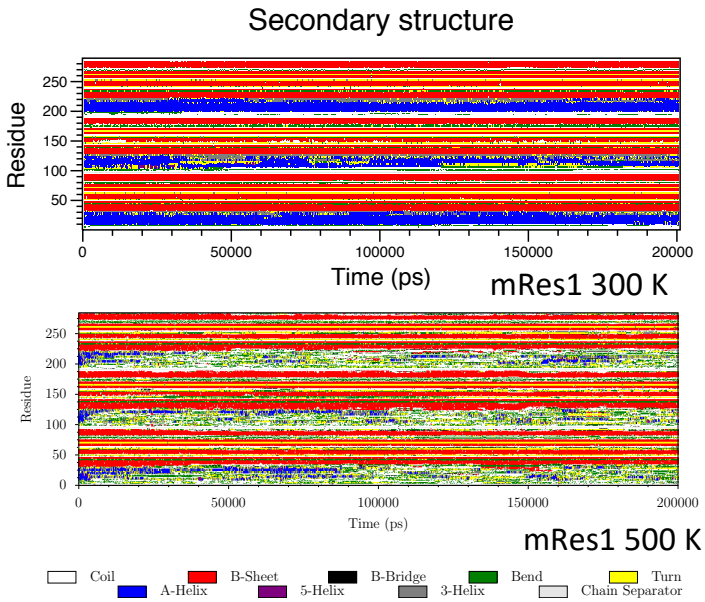

Figure 23: Secondary structural fluctuations of mRes2 at a) 300 K and b) 500 K. Trimer form.

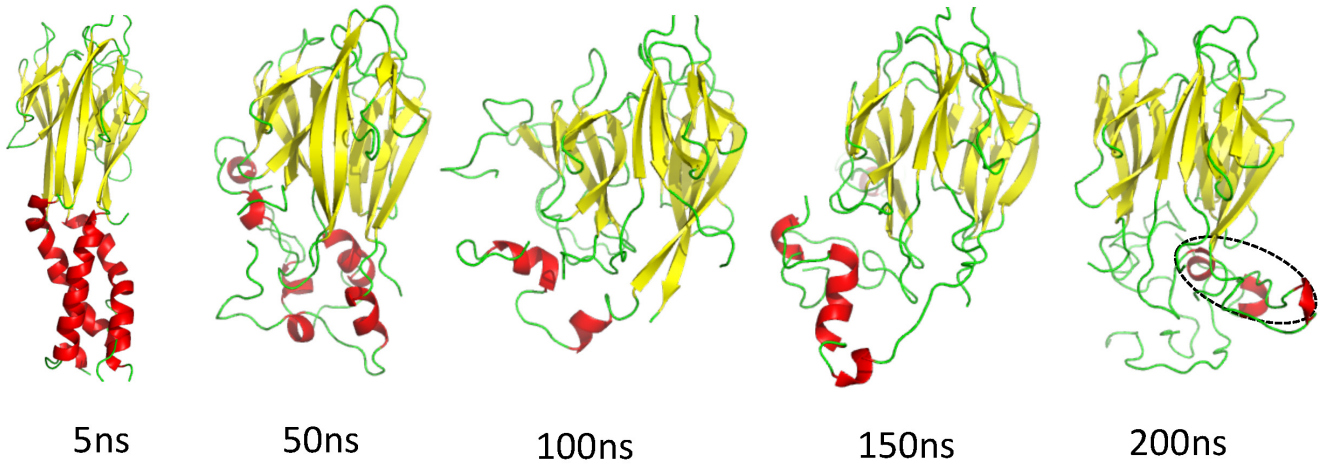

Figure 24: Snapshots every 50 ns of the simulation at 500 K for mRes2.

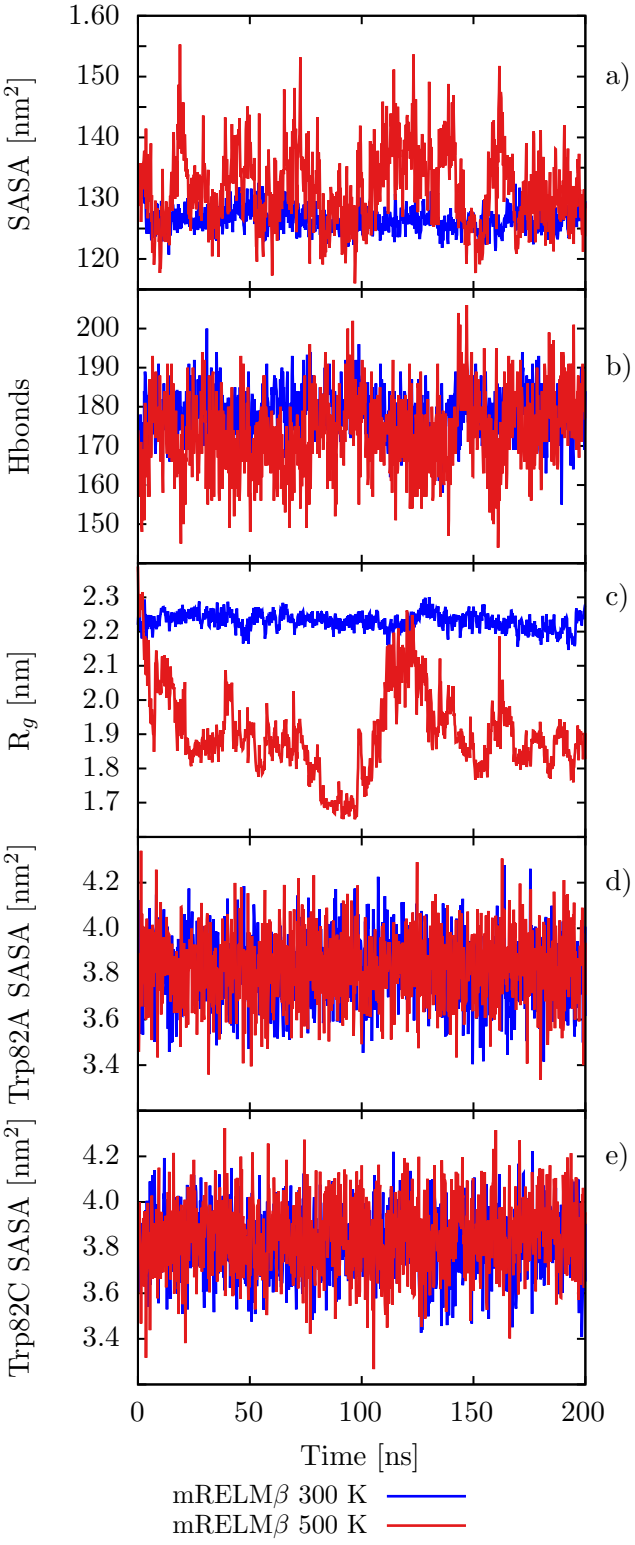

Figure 25: mRELMβ characteristics at two temperatures. a) Protein SASA, b) H_{bonds}, c) protein compactness, d) Trp82A SASA and e) Trp82C and SASA. Trimer form.

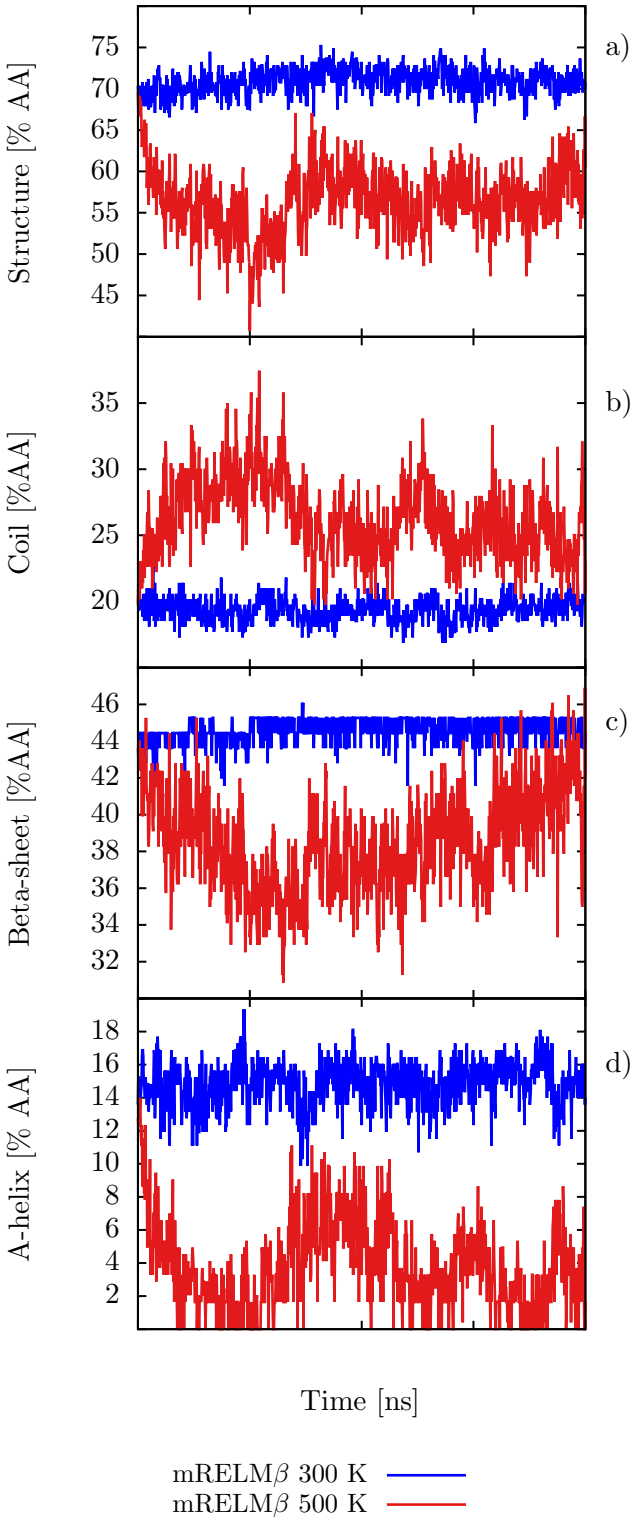

Figure 26: mRELMβ at two temperatures. a) Protein Structure = α-Helix + β-Sheet + β-Bridge + Turn, b) Coil, c) β-Sheet, d) α-Helix. T= 300K. Trimer form.

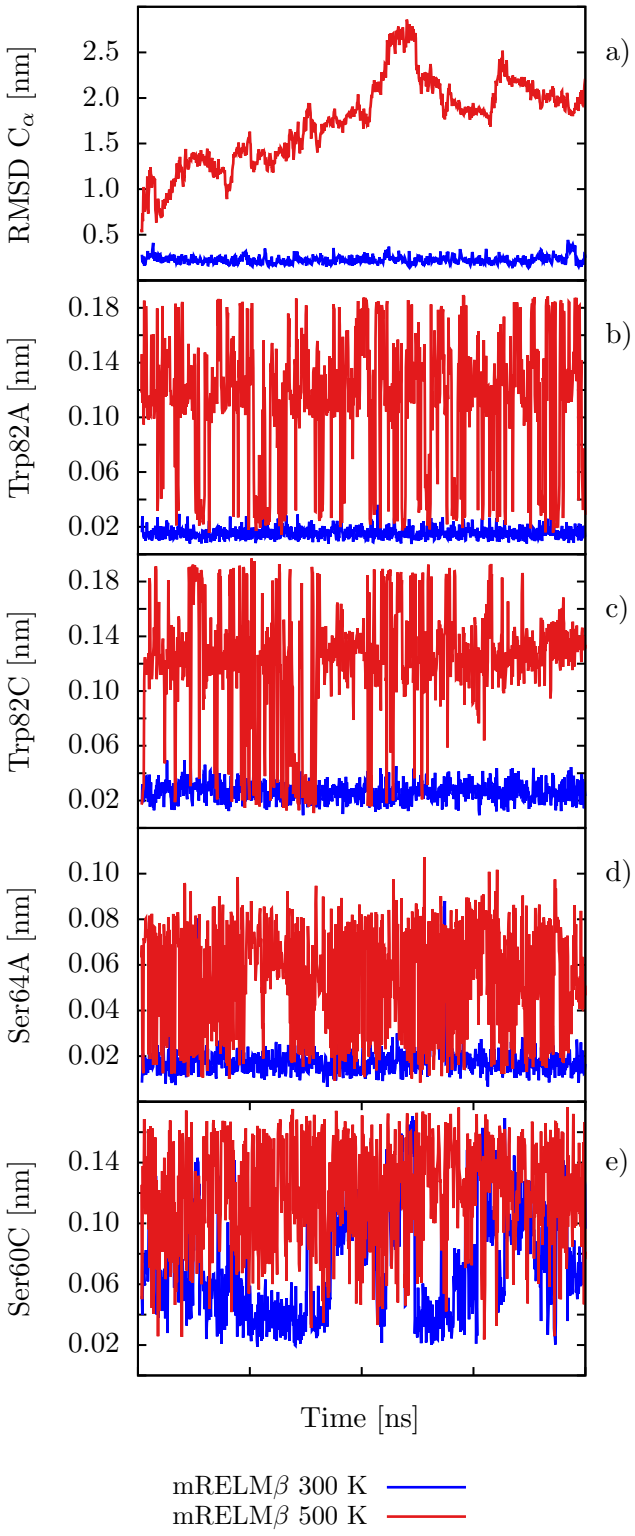

Figure 27: mRELMβ at two temperatures. a) RMSD of Cα, b) Trp82A, c) Trp82C, d) Ser64A and e) Ser60C. T= 300K. Trimer form. Here, AA means amino acid.

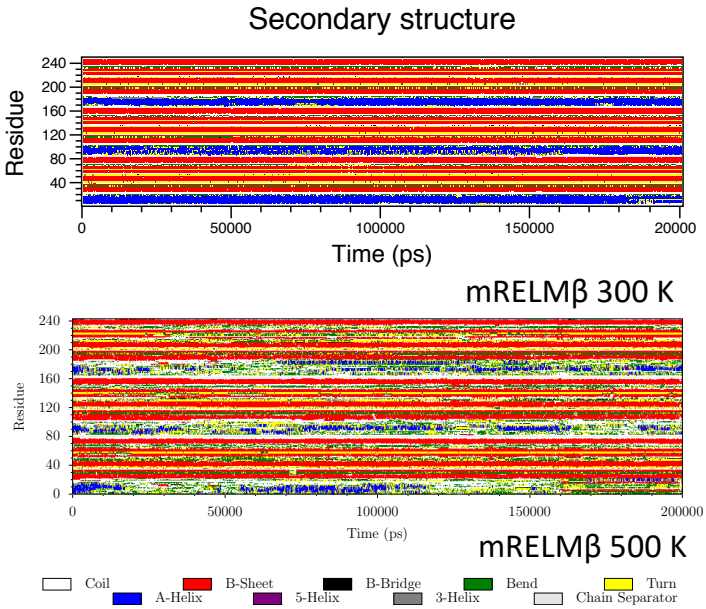

Figure 28: . Secondary structural fluctuations of mRELMβ at a) 300 K and b) 500 K. Trimer form.

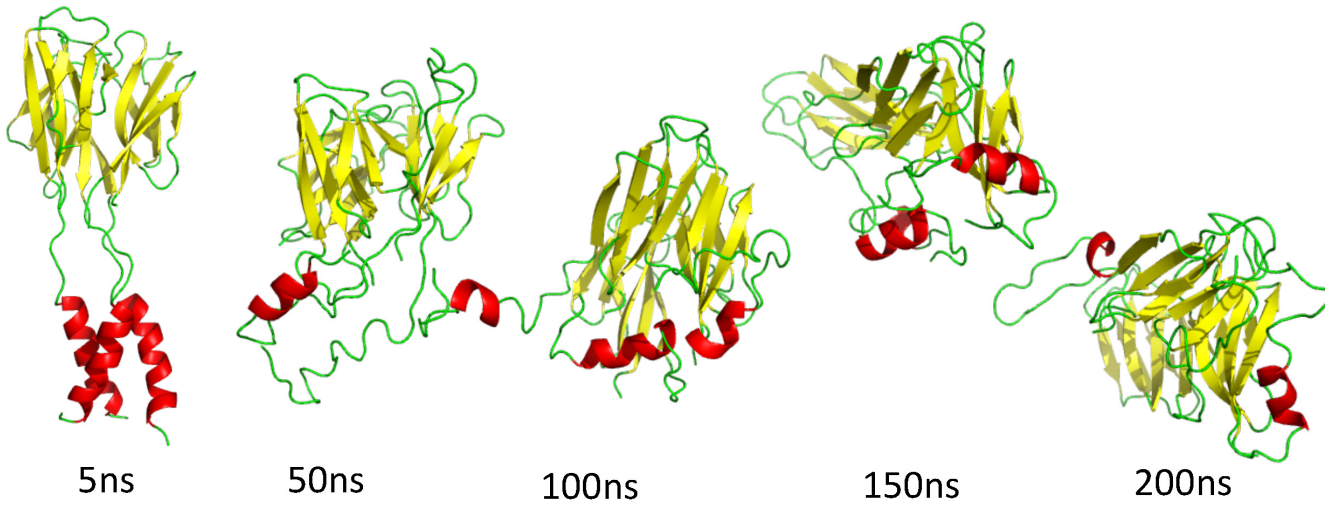

Figure 29: Snapshots every 50 ns of the simulation at 500 K for mRELMβ.

4.5 Conclusions

Acording to estimations, mRes1 is the structure with the largest average SASA value throughout the simulations, followed by mRes2 and finally mRELMβ.

The two crystal structures reported in PDB for mourine resistin share the same primary sequence but different secondary structure. Here, we found that mRes1 present a more open globular domain that is preserved the majority of the 200 ns at 300 K, compared with mRes2 or its homologue mRELMβ.

The propensity to interconvert α-helices into turns, 3-5-Helix or coil parts is common to the mRes(1-2) and mRELMβ at 300 K and it affects different chains in different proteins.

We found that in all the RELMs studied here, there is a lost of helicity as a first step of denaturation. There is a high stability of the globular β-sheet domain in resistin protein that does not appears in RELMβ protein.

At 500 K we found a partially interconversion of α-helices into β-sheets in all proteins, indicating that this propensity is not only found during agregation but also during heating.

We had been able to identify a largely persistent hydrogen-bond network shared by all the proteins in the interchain globular domain at room temperature. This hydrogen-bond network is considerably conserved at elevated temperature in mRes(1-2) but not in mRELMβ.

4.6 acknowledgments

We acknowledge the use of the clusters Xiuhcoatl and ABACUS at CINVESTAV.

References

[1] Claire M Steppan, Elizabeth J Brown, Christopher M Wright, Savitha Bhat, Ronadip R Banerjee, Charlotte Y Dai, Gregory H Enders, Debra G Silberg, Xiaoming Wen, Gary D Wu, et al. A family of tissue-specific resistin-like molecules. *Proceedings of the National Academy of Sciences*, 98(2):502–506, 2001.

[2] Zhongji Meng, Yonghong Zhang, Zhiqiang Wei, Ping Liu, Jian Kang, Yinhua Zhang, Deqiang Ma, Changzheng Ke, Yue Chen, Jie Luo, et al. High serum resistin associates with intrahepatic inflammation and necrosis: an index of disease severity for patients with chronic hbv infection. *BMC gastroenterology*, 17(1):6, 2017.

[3] Meera G Nair, Yurong Du, Jacqueline G Perrigoue, Colby Zaph, Justin J Taylor, Michael Goldschmidt, Gary P Swain, George D Yancopoulos, David M Valenzuela, Andrew Murphy, et al. Alternatively activated macrophage-derived relm-α is a negative regulator of type 2 inflammation in the lung. *Journal of Experimental Medicine*, 206(4):937–952, 2009.

[4] Hye Seung Jung, Ki-Ho Park, Young Min Cho, Sung Soo Chung, Hyun Ju Cho, Soo Youn Cho, Sang Joon Kim, Seong Yeon Kim, Hong Kyu Lee, and Kyong Soo Park. Resistin is secreted from macrophages in atheromas and promotes atherosclerosis. *Cardiovascular research*, 69(1):76–85, 2006.

[5] J. Malyszko, J.S. Malyszko, K. Pawlak, and M. Mysliwiec. Resistin, a new adipokine, is related to inflammation and renal function in kidney allograft recipients. *Transplantation Proceedings*, 38(10):3434–3436, 2006.

[6] Lisa C Osborne, Karen L Joyce, Theresa Alenghat, Gregory F Sonnenberg, Paul R Giacomin, Yurong Du, Kirk S Bergstrom, Bruce A Vallance, and Meera G Nair. Resistin-like molecule α promotes pathogenic th17 cell responses and bacterial-induced intestinal inflammation. *The Journal of Immunology*, page 1200706, 2013.

[7] Wei-kai Hou, Yu-xin Xu, Ting Yu, Li Zhang, Wen-wen Zhang, Chun-li Fu, Yu Sun, Qing Wu, and Li Chen. Adipocytokines and breast cancer risk. *Chinese medical journal*, 120(18):1592–1596, 2007.

[8] Ales Smekal and Jan Vaclavik. Adipokines and cardiovascular disease: A comprehensive review. *Biomedical Papers of the Medical Faculty of Palacky University in Olomouc*, 161(1), 2017.

[9] A Stofkova. Resistin and visfatin: regulators of insulin sensitivity, inflammation and immunity. *Endocrine regulations*, 44(1):25–36, 2010.

[10] Akshay Sood and Stephanie A Shore. Adiponectin, leptin, and resistin in asthma: basic mechanisms through population studies. *Journal of allergy*, 2013, 2013.

[11] Akifumi Kushiyama, Nobuhiro Shojima, Takehide Ogihara, Kouichi Inukai, Hideyuki Sakoda, Midori Fujishiro, Yasushi Fukushima, Motonobu Anai, Hiraku Ono, Nanao Horike, et al. Resistin-like molecule β activates mapks, suppresses insulin signaling in hepatocytes, and induces diabetes, hyperlipidemia, and fatty liver in transgenic mice on a high fat diet. *Journal of Biological Chemistry*, 280(51):42016–42025, 2005.

[12] Evan D Muse, Silvana Obici, Sanjay Bhanot, Brett P Monia, Robert A McKay, Michael W Rajala, Philipp E Scherer, and Luciano Rossetti. Role of resistin in diet-induced hepatic insulin resistance. *The Journal of clinical investigation*, 114(2):232–239, 2004.

[13] Gabrielle M Pine, Hashini M Batugedara, and Meera G Nair. Here, there and everywhere: Resistin-like molecules in infection, inflammation, and metabolic disorders. *Cytokine*, 2018.

[14] Mária Filková, Martin Haluzík, Steffen Gay, and Ladislav Šenolt. The role of resistin as a regulator of inflammation: Implications for various human pathologies. *Clinical immunology*, 133(2):157–170, 2009.

[15] Miguel Patrício, José Pereira, Joana Crisóstomo, Paulo Matafome, Manuel Gomes, Raquel Seiça, and Francisco Caramelo. Using resistin, glucose, age and bmi to predict the presence of breast cancer. *BMC cancer*, 18(1):29, 2018.

[16] Yitang Sun, Jingqi Zhou, and Kaixiong Ye. Prioritizing causal risk factors for severe covid-19: An exhaustive mendelian randomization study. 2021.

[17] MGS Shashaty, TA Miano, CV Cosgriff, TK Jones, HM Giannini, O Oniyide, AR Weisman, C Ittner, T Dunn, RS Agyekum, et al. Plasma resistin levels are associated with acute kidney injury in hospitalized covid-19 patients. In *TP50. TP050 COVID: NONPULMONARY CRITICAL CARE, MECHANICAL VENTILATION, BEHAVIORAL SCIENCES, AND EPI*, pages A2571–A2571. American Thoracic Society, 2021.

[18] Claire M Steppan, Shannon T Bailey, Savitha Bhat, Elizabeth J Brown, Ronadip R Banerjee, Christopher M Wright, Hiralben R Patel, Rexford S Ahima, and Mitchell A Lazar. The hormone resistin links obesity to diabetes. *Nature*, 409(6818):307, 2001.

[19] Syeda Ijlal Zehra Zaidi and Tanvir Ali Khan Shirwany. Relationship of serum resistin with insulin resistance and obesity. *Journal of Ayub Medical College Abbottabad*, 27(3):552–555, 2015.

[20] Koichiro Azuma, Fuminori Katsukawa, Shuji Oguchi, Mitsuru Murata, Hajime Yamazaki, Akira Shimada, and Takao Saruta. Correlation between serum resistin level and adiposity in obese individuals. *Obesity research*, 11(8):997–1001, 2003.

[21] KM Utzschneider, DB Carr, J Tong, TM Wallace, RL Hull, S Zraika, Q Xiao, JS Mistry, BM Retzlaff, RH Knopp, et al. Resistin is not associated with insulin sensitivity or the metabolic syndrome in humans. *Diabetologia*, 48(11):2330–2333, 2005.

[22] Ivan Nagaev and Ulf Smith. Insulin resistance and type 2 diabetes are not related to resistin expression in human fat cells or skeletal muscle. *Biochemical and biophysical research communications*, 285(2):561–564, 2001.

[23] Heshen Tian, Lei Liu, Ying Wu, Ruiwen Wang, Yongliang Jiang, Ruicheng Hu, Liming Zhu, Linwei Li, Yanyan Fang, Chulan Yang, et al. Resistin-like molecule β acts as a mitogenic factor in hypoxic pulmonary hypertension via the ca^{2+} - dependent pi3k/akt/mtor and pkc/mapk signaling pathways. *Respiratory Research*, 22(1):1–20, 2021.

[24] Claire M Steppan and Mitchell A Lazar. The current biology of resistin. *Journal of internal medicine*, 255(4):439–447, 2004.

[25] KM Barnes and JL Miner. Role of resistin in insulin sensitivity in rodents and humans. *Current Protein and Peptide Science*, 10(1):96–107, 2009.

[26] Fatima Al Hannan and Kevin Gerard Culligan. Human resistin and the relm of inflammation in diabesity. *Diabetology & metabolic syndrome*, 7(1):54, 2015.

[27] David B Savage, Ciaran P Sewter, Ellen S Klenk, David G Segal, Antonio Vidal-Puig, Robert V Considine, and Stephen O'Rahilly. Resistin/fizz3 expression in relation to obesity and peroxisome proliferator–activated receptor-γ action in humans. *Diabetes*, 50(10):2199–2202, 2001.

[28] Saurabh D Patel, Michael W Rajala, Luciano Rossetti, Philipp E Scherer, and Lawrence Shapiro. Disulfide-dependent multimeric assembly of resistin family hormones. *Science*, 304(5674):1154–1158, 2004.

[29] Sahmin Lee, Hyun-Chae Lee, Yoo-Wook Kwon, Sang Eun Lee, Youngjin Cho, Joonoh Kim, Soobeom Lee, Ju-Young Kim, Jaewon Lee, Han-Mo Yang, et al. Adenylyl cyclase-associated protein 1 is a receptor for human resistin and mediates inflammatory actions of human monocytes. *Cell metabolism*, 19(3):484–497, 2014.

[30] Madhuri Suragani, Varma D Aadinarayana, Aleem Basha Pinjari, Karunakar Tanneeru, Lalitha Guruprasad, Sharmistha Banerjee, Saurabh Pandey, Tapan K Chaudhuri, and Nasreen Zafar Ehtesham. Human resistin, a proinflammatory cytokine, shows chaperone-like activity. *Proceedings of the National Academy of Sciences*, 110(51):20467–20472, 2013.

[31] L América Chi and M Cristina Vargas. In silico design of peptides as potential ligands to resistin. *Journal of molecular modeling*, 26(5):1–14, 2020.

[32] Helen M Berman, John Westbrook, Zukang Feng, Gary Gilliland, Talapady N Bhat, Helge Weissig, Ilya N Shindyalov, and Philip E Bourne. The protein data bank. *Nucleic acids research*, 28(1):235–242, 2000.

[33] Xavier Robert and Patrice Gouet. Deciphering key features in protein structures with the new endscript server. *Nucleic acids research*, 42(W1):W320–W324, 2014.

[34] Beatriz Sánchez-Solana, Jorge Laborda, and Victoriano Baladrón. Mouse resistin modulates adipogenesis and glucose uptake in 3t3-l1 preadipocytes through the ror1 receptor. *Molecular endocrinology*, 26(1):110–127, 2012.

[35] Alexes C Daquinag, Yan Zhang, Felipe Amaya-Manzanares, Paul J Simmons, and Mikhail G Kolonin. An isoform of decorin is a resistin receptor on the surface of adipose progenitor cells. *Cell stem cell*, 9(1):74–86, 2011.

[36] Andrej Tarkowski, Jan Bjersing, Andrey Shestakov, and Maria I Bokarewa. Resistin competes with lipopolysaccharide for binding to toll-like receptor 4. *Journal of cellular and molecular medicine*, 14(6b):1419–1431, 2010.

[37] Hiroshi Onuma, Yasuharu Tabara, Ryoichi Kawamura, Jun Ohashi, Wataru Nishida, Yasunori Takata, Masaaki Ochi, Tatsuya Nishimiya, Ryuichi Kawamoto, Katsuhiko Kohara, et al. Plasma resistin is associated with single nucleotide polymorphisms of a possible resistin receptor, the decorin gene, in the general japanese population. *Diabetes*, 62(2):649–652, 2013.

[38] Ronadip R Banerjee and Mitchell A Lazar. Dimerization of resistin and resistin-like molecules is determined by a single cysteine. *Journal of Biological Chemistry*, 276(28):25970–25973, 2001.

[39] Battu Aruna, Sudip Ghosh, Anil K Singh, Shekhar C Mande, V Srinivas, Radha Chauhan, and Nasreen Z Ehtesham. Human recombinant resistin protein displays a tendency to aggregate by forming intermolecular disulfide linkages. *Biochemistry*, 42(36):10554–10559, 2003.

[40] David Van Der Spoel, Erik Lindahl, Berk Hess, Gerrit Groenhof, Alan E Mark, and Herman JC Berendsen. Gromacs: fast, flexible, and free. *Journal of computational chemistry*, 26(16):1701–1718, 2005.

[41] Kresten Lindorff-Larsen, Stefano Piana, Kim Palmo, Paul Maragakis, John L Klepeis, Ron O Dror, and David E Shaw. Improved side-chain torsion potentials for the amber ff99sb protein force field. *Proteins: Structure, Function, and Bioinformatics*, 78(8):1950–1958, 2010.

[42] Herman JC Berendsen, JPM van Postma, Wilfred F van Gunsteren, ARHJ DiNola, and JR Haak. Molecular dynamics with coupling to an external bath. *The Journal of chemical physics*, 81(8):3684–3690, 1984.

[43] Tom Darden, Darrin York, and Lee Pedersen. Particle mesh ewald: An nlog (n) method for ewald sums in large systems. *The Journal of chemical physics*, 98(12):10089–10092, 1993.

[44] Berk Hess, Henk Bekker, Herman JC Berendsen, and Johannes GEM Fraaije. Lincs: a linear constraint solver for molecular simulations. *Journal of computational chemistry*, 18(12):1463–1472, 1997.

[45] MSKP Settle. An analytical version of the shake and rattle algorithm for rigid water molecules. *J. Comput. Chem*, 13:952–962, 1992.

[46] Xavier Daura, Karl Gademann, Bernhard Jaun, Dieter Seebach, Wilfred F van Gunsteren, and Alan E Mark. Peptide folding: when simulation meets experiment. *Angewandte Chemie International Edition*, 38(1-2):236–240, 1999.

[47] Jack Kyte and Russell F Doolittle. A simple method for displaying the hydropathic character of a protein. *Journal of molecular biology*, 157(1):105–132, 1982.

[48] Chi-Chang Juan, Lou-Sing Kan, Cheng-Chih Huang, Shih-Shih Chen, Low-Tone Ho, and Lo-Chun Au. Production and characterization of bioactive recombinant resistin in escherichia coli. *Journal of biotechnology*, 103(2):113–117, 2003.